



Polysaccharide Succinylation Enhances the Intracellular Survival of *Mycobacterium abscessus*

Zuzana Palčková, Martine Gilleron, Shiva Kumar Angala, Juan Manuel Belardinelli, Michael Mcneil, Luiz Bermudez, Mary Jackson

► To cite this version:

Zuzana Palčková, Martine Gilleron, Shiva Kumar Angala, Juan Manuel Belardinelli, Michael Mcneil, et al.. Polysaccharide Succinylation Enhances the Intracellular Survival of *Mycobacterium abscessus*. *ACS Infectious Diseases*, 2020, 6 (8), pp.2235-2248. <10.1021/acsinfecdis.0c00361>. <hal-03008493>

HAL Id: hal-03008493

<https://hal.science/hal-03008493v1>

Submitted on 18 Nov 2020

HAL is a multi-disciplinary open access archive for the deposit and dissemination of scientific research documents, whether they are published or not. The documents may come from teaching and research institutions in France or abroad, or from public or private research centers.

L'archive ouverte pluridisciplinaire **HAL**, est destinée au dépôt et à la diffusion de documents scientifiques de niveau recherche, publiés ou non, émanant des établissements d'enseignement et de recherche français ou étrangers, des laboratoires publics ou privés.



HAL Authorization

Polysaccharide Succinylation Enhances the Intracellular Survival of *Mycobacterium abscessus*

Zuzana Palčková, Martine Gilleron, Shiva Kumar Angala, Juan Manuel Belardinelli, Michael McNeil, Luiz E. Bermudez, and Mary Jackson*



Cite This: <https://dx.doi.org/10.1021/acsinfecdis.0c00361>



Read Online

ACCESS |



Metrics & More



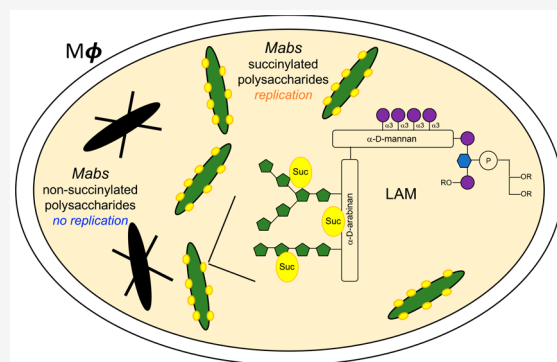
Article Recommendations



Supporting Information

ABSTRACT: Lipoarabinomannan (LAM) and its biosynthetic precursors, phosphatidylinositol mannosides (PIMs) and lipomannan (LM) play important roles in the interactions of *Mycobacterium tuberculosis* with phagocytic cells and the modulation of the host immune response, but nothing is currently known of the impact of these cell envelope glycoconjugates on the physiology and pathogenicity of nontuberculous mycobacteria. We here report on the structures of *Mycobacterium abscessus* PIM, LM, and LAM. Intriguingly, these structures differ from those reported previously in other mycobacterial species in several respects, including the presence of a methyl substituent on one of the mannosyl residues of PIMs as well as the PIM anchor of LM and LAM, the size and branching pattern of the mannan backbone of LM and LAM, and the modification of the arabinan domain of LAM with both succinyl and acetyl substituents. Investigations into the biological significance of some of these structural oddities point to the important role of polysaccharide succinylation on the ability of *M. abscessus* to enter and survive inside human macrophages and epithelial cells and validate for the first time cell envelope polysaccharides as important modulators of the virulence of this emerging pathogen.

KEYWORDS: *Mycobacterium abscessus*, nontuberculous mycobacteria, lipoarabinomannan, arabinogalactan, succinylation



The prevalence of pulmonary nontuberculous mycobacterial (NTM) infections caused by *Mycobacterium abscessus* complex (MABSC) species including *M. abscessus* subsp. *abscessus* [Mabs], *M. abscessus* subsp. *massiliense*, and *M. abscessus* subsp. *bolletii* is increasing worldwide, disproportionately affecting patients with structural lung disease such as chronic obstructive pulmonary disease (COPD), bronchiectasis, and cystic fibrosis (CF).^{1–4} The intrinsic recalcitrance of MABSC to chemotherapeutic treatments and alarming treatment failure rates (in the range of 42 to 75%)⁵ place a high priority on the development of more effective treatment approaches, a goal that may only be achieved with a better understanding of MABSC chronic infections and of the bacteria and host-related factors responsible for drug resistance and disease progression.

The distinctive cell envelope of mycobacteria is a key modulator of their interactions with the host during infection.^{6,7} Yet, with the exception of surface glycopeptidolipids which have been shown to impact the biofilm-forming capacity and pathogenicity of MABSC, studies on the contribution of cell envelope constituents to NTM infections have thus far been very limited.^{8–14} A group of glycolipids known as the trehalose polyphosphates was recently proposed to contribute to the hyper-aggregative phenotype of rough

MABSC variants.¹⁵ A screen based on the survival of Mabs transposon mutants inside amoebae and macrophages has further led to the discovery of an ESX-4 type VII secretion system and of a partially characterized family of glycolipids as modulators of the intracellular survival of Mabs.^{16,17} Despite their critical contribution to the interactions of *Mycobacterium tuberculosis* with phagocytic and nonphagocytic cells and to immunomodulation in the course of tuberculosis, the impact of lipomannan (LM), lipoarabinomannan (LAM), and metabolic glycolipid precursors, phosphatidylinositol mannosides (PIM), in the pathogenicity of NTM has not yet been investigated.^{18–20} That cell envelope (lipo)polysaccharides may contribute to NTM virulence was first suggested by Yamazaki et al.,²¹ who reported on a *Mycobacterium avium* transposon mutant impaired in biofilm formation whose virulence in mice and ability to invade bronchiolar epithelial cells were significantly reduced. Although unknown at the time, the

Received: May 26, 2020

Published: July 13, 2020



ACS Publications

© XXXX American Chemical Society

A

<https://dx.doi.org/10.1021/acsinfecdis.0c00361>
ACS Infect. Dis. XXXX, XXX, XXX–XXX

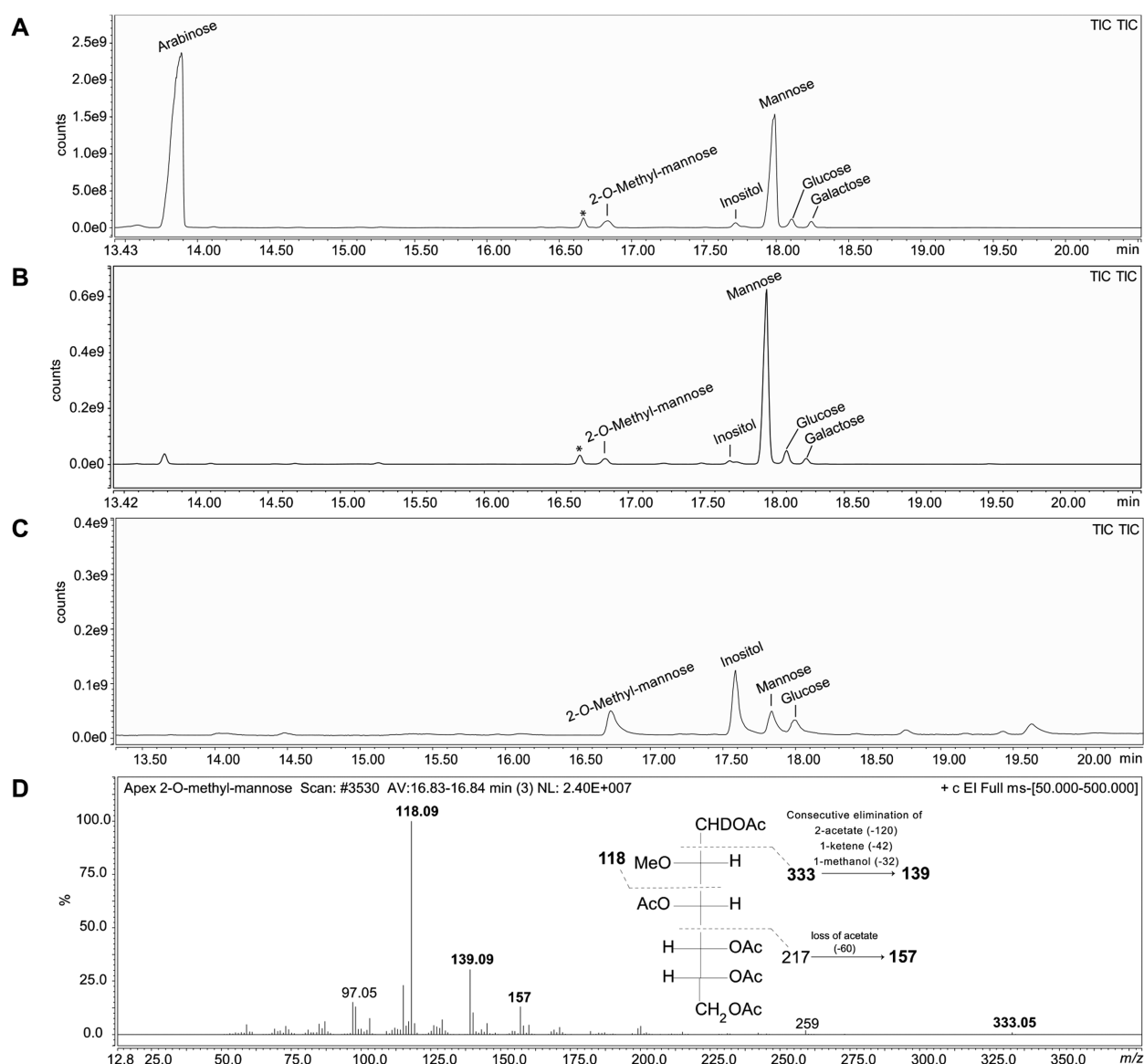


Figure 1. Monosaccharidic composition of LAM, LM, and phosphatidylinositol dimannosides from WT *Mabs* ATCC 19977. GC/MS analysis of alditol acetate derivatives prepared from WT *Mabs* LAM (A), LM (B) and PIM₂ (C). (D) Extracted ion mass spectrum and structure corresponding to the peak identified as 2-O-methylmannose with retention time 16.83 min and characteristic ions with *m/z* 118, 139, 157, and 333. This peak was detected in all three samples. *Noncarbohydrate contaminant.

transposon harbored by this mutant had disrupted a conserved gene named *sucT* which our recent work in *Mycobacterium smegmatis* established to be responsible for the succinylation of two major (lipo)polysaccharides of the mycobacterial cell envelope: arabinogalactan (AG) and LAM.²² While the biological significance of AG and LAM succinylation remains unclear, it was recently shown that the prevalence of succinyl residues on *M. tuberculosis* LAM increased during host infection.²³

With the goal of gaining insights into the contribution of MABSC's cell envelope polysaccharides to pathogenicity, we first report on the structural characterization of PIM, LM, and LAM from *Mabs* ATCC 19977 and on the unique features that distinguish these molecules from those isolated previously from other mycobacteria. Using a *sucT*-deficient mutant of the same *Mabs* isolate generated herein, we next provide the first unequivocal evidence of the involvement of cell envelope (lipo)polysaccharides in the virulence of MABSC.

RESULTS

Structural Characterization of LM and LAM from *Mabs*. Overall Organization of Mycobacterial LM and LAM. Since the structures of *Mabs* LM and LAM had never been previously reported, we first undertook to characterize these structures and to compare them to those of *Mtb* and other NTM. The lipid component of LM and LAM is a mannosylated phosphatidyl-*myo*-inositol moiety that serves to anchor the lipoglycans in the inner and outer membranes of the cell envelope²⁴ [see further in the text for a representation of LAM]. Extending from this anchor and common to LM and LAM is a linear $\alpha(1 \rightarrow 6)$ -linked mannan backbone made up of 20–25 mannosyl units which are $\alpha(1 \rightarrow 2)$ -linked in the case of *M. tuberculosis* and *M. smegmatis*, but $\alpha(1 \rightarrow 3)$ -linked in the case of *M. chelonae*, a *Mycobacterium* species closely related to *Mabs*.²⁵ In LAM, a single D-arabinan chain consisting of ~60 arabinofuranose (Araf) residues is further attached to the

mannan backbone.²⁶ The arabinan domain of LAM is very similar to that of AG and made of stretches of $\alpha(1 \rightarrow 5)$ -linked Ara_f residues with precisely positioned $\alpha(3 \rightarrow 5)$ -branch sites. The nonreducing termini of the D-arabinan domain consist of a branched Ara₆ motif as found in AG or of a linear Ara₄.^{27,28} Key to the biological activity of the entire LAM molecule is the species-specific structural microheterogeneity that typifies its nonreducing arabinan termini. Whereas *M. tuberculosis* and some other pathogenic slow-growing mycobacteria produce a mannoside-capped LAM (designated ManLAM), some fast-growing NTM species (e.g., *M. smegmatis* and *M. fortuitum*) instead harbor phosphoinositol caps, yielding PI-LAM, while some others are devoid of caps altogether (e.g., *M. chelonae*).^{29,30} Finally, we note the presence of succinyl residues modifying the C2 position of a portion of the internal α -3,5-branched Ara_f residues as well as quantitatively minor α -1,5-Ara_f positions of the arabinan domains of AG and LAM from *M. tuberculosis*, *M. bovis* BCG and *M. smegmatis*,^{22,28,31–33} in addition to succinyl residues modifying the C3 position of β -(1 \rightarrow 2)-linked Ara_f residues of the nonreducing arabinan termini of LAM in *M. tuberculosis*.²³ Intriguingly, in *M. kansasii*, succinates were found to substitute the C3 position of linear α -1,5-Ara_f residues rather than the internal α -3,5-branched Ara_f residues of LAM.³⁴

Characterization of the Mannan Domain of *Mabs* LM and LAM. In order to elucidate the structure of the *Mabs* lipoglycans, we first focused on the characterization of their glycosyl composition. The glycosyl composition of LM and LAM is presented in Figure 1 and Table S1. The expected arabinose to mannose ratios were found in LAM. Surprisingly, small amounts of 2-O-methyl (2-O-Me) hexose presumed to be 2-O-Me mannose were seen in both LAM and LM, as well as in phosphatidylinositol dimannosides, as will be discussed further [Figure 1A–D]. The glycosyl linkage composition of LAM and LM is shown in Table S2. We note that, like in the LAM and LM of *M. chelonae*, the dominant branched mannosyl residue is 3,6-Man_p rather than 2,6-Man_p. This observation was also obvious from the NMR analysis of LM and LAM. The anomeric proton region of *Mabs* LM 1D ¹H spectrum is dominated by two signals at 5.12 and 4.87 ppm [Figure 2B] correlating with two carbons at 105.10 and 102.15 ppm, respectively [Figure 2B]. While the former signal correlates in the TOCSY with a single H-2 at 4.06 ppm, the other correlates with two largely distinct H-2 signals at 3.97 and 4.12 ppm (not shown) indicating the presence of two anomeric protons at 4.87 ppm. The three spin systems were assigned to *t*-Man_p (IV), 6-Man_p (VI), and 3,6-Man_p (VIII) [Table 1] in accordance with published literature.^{25,33,35–37} The same three spin systems (IV, VI, VIII) were also observed in the ¹H–¹³C HMQC of LAM [Figure 2A]. No 2,6-Man_p could be observed by NMR despite small amounts being detected by glycosyl linkage analysis [Table S2] suggesting that the 2,6-Man_p identified with the latter method was in fact undermethylated 6-Man_p.

The mass spectrum of deacylated *Mabs* LM [Figure 3A] showed that its size was considerably bigger than that of *M. smegmatis* LM, which averages 23–29 residues,³⁸ in that *Mabs* LM averaged 32–44 mannosyl residues. LM with an even number of mannosyl residues also predominated, although significant amounts of LM with an odd number of mannosyl residues was also present. Intriguingly, after digestion with α -1,6-endomannanase from *Bacillus circulans* TN-31,³⁸ large mannans (free from the reducing mannosylated

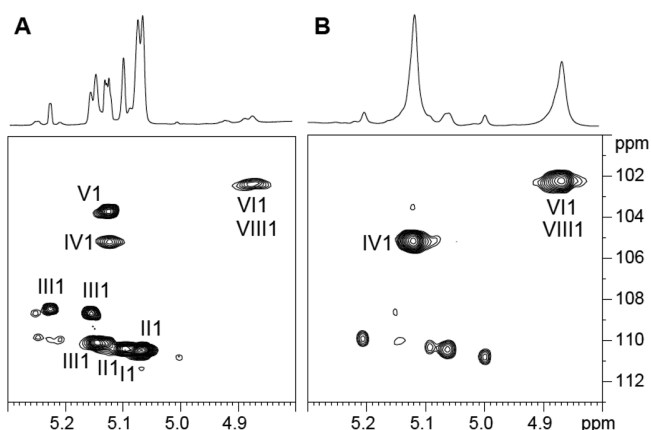


Figure 2. Branching of the mannan domain of LM and LAM from *Mabs* ATCC 19977. Expanded region (δ ¹H: 4.80–5.30, δ ¹³C 100–113) of the 2D ¹H–¹³C HMQC spectrum in D₂O at 298 K of LAM (A) and LM (B) from WT *Mabs* ATCC 19977. I, 3,5 α -Ara_f; II, 5 α -Ara_f; III, 2 α -Ara_f; IV, *t*- α Man_p; V, β -Ara_f; VI, 6 α Man_p; VIII, 3,6 α Man_p. The nomenclature used is as described in ref 25.

phosphatidyl-*myo*-inositol moiety) were produced and they were all of even masses [Figure 3B]. The large mannans were approximately six mannosyl residues shorter than the intact *Mabs* LM suggesting a region of nonbranched α -1,6-linked mannosyl residues next to the inositol as in the mannan from *M. smegmatis* LM.³⁸ A Man₄ tetrasaccharide was also released in large amounts upon endomannanase digestion [Figure 3C]. It cannot be a linear α -1,6-linked mannosyl tetrasaccharide or it would have been further degraded by the enzyme. It must thus reflect the mannan branching pattern but both its structure and its location on the mannan backbone remain to be elucidated.

Characterization of the Lipid Anchor of *Mabs* LM and LAM. GC/MS analysis of fatty acid methyl esters prepared from WT *Mabs* LM and LAM revealed the presence of C14:0 and C15:0 besides the fatty acids typically found esterifying the lipid anchor of *M. tuberculosis* or *M. smegmatis* LM and LAM (C16:0, C18:0, C18:1, tuberculostearic acid) [Table S3]. Thus, similar to *M. chelonae*, the lipid anchor of *Mabs* LM and LAM is acylated with a greater variety of fatty acids than typically seen in *M. tuberculosis*.³⁹ Unlike the situation in *M. chelonae*,²⁵ however, the relative distribution of fatty acids differed between LM and LAM. Whereas C16:0 was the most abundant fatty acid found in both lipoglycans (representing 36.2 and 66% of the total fatty acid content of WT LM and LAM, respectively), comparable amounts of C18:0 (32.9%) was found in LM whereas in LAM, C18:0 only represented ~9% of the total fatty acids. Conversely, more C14:0 was found esterifying the lipid anchor of WT LAM than WT LM (14% vs 0.9%).

We next sought to elucidate the origin of the 2-O-Me hexose residues identified in LM and LAM [Figure 1A,B,D]. Since this residue was also found on purified phosphatidylinositol dimannosides [Figure 1C], we believed that the methyl group is located on a Man_p residue of the phosphatidylinositol anchor. In support of this hypothesis, LC/MS analysis of deacylated *Mabs* LM indicated that each LM species was 14 mass units higher than predicted from its component parts [Figure 3A] suggesting that all molecules of the LM contained the 2-O-Me mannosyl residue. To map its location, deacylated *Mabs* LM was next digested with α -1,6-endomannanase. The

Table 1. ^1H and ^{13}C NMR Chemical Shifts of LM from WT *Mabs* ATCC 19977 Measured at 298 K in D_2O

		1	2	3	4	5	6
<i>t</i> Manp	^{13}C	105.1	72.99	73.65	69.70	76.20	63.90
	^1H	5.12	4.06	3.86	3.65	3.76	3.76/3.87
6Manp	^{13}C	102.15	72.44	73.65	69.70	nd	69.65
	^1H	4.87	3.97	3.86	3.65	nd	3.76/3.88
3,6Manp	^{13}C	102.15	72.86	81.29	68.79	73.34	68.24
	^1H	4.87	4.12	3.91	3.86	3.87	3.75/3.94

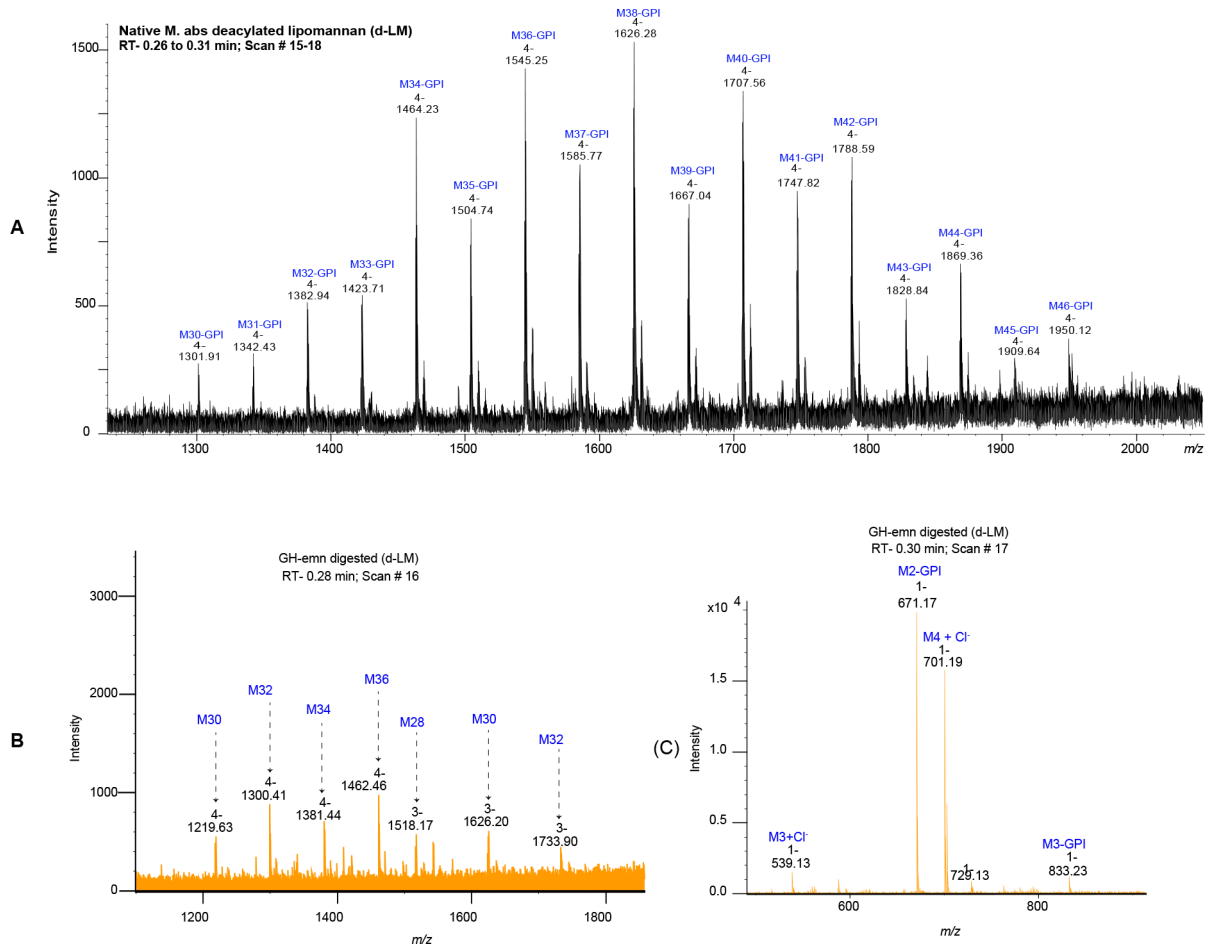


Figure 3. Negative ion liquid chromatography–mass spectrometry (LC-MS) analysis of the *Mabs* deacylated LM (d-LM) before and after digestion with α -1,6-endomannanase (GH-emn). (A) LC-MS profile of *Mabs* d-LM before enzymatic treatment. The mass spectrum is dominated by a series of quadruply charged ions corresponding to the high molecular weight mannan backbone containing 30 to 46 mannosyl residues [M30 to M46] (range of 5000 to 7800 Da). (B,C) LC-MS profile of *Mabs* d-LM after treatment with the GH-emn α -1,6-endomannanase. The mass spectrum at 0.28 min retention time (B) corresponds to oligomannans (lacking the glycerol-phosphatidyl inositol anchor [GPI]) with an even number of mannosyl residues from M28 to M36. The mass spectrum at 0.30 min retention time (C) shows two major ions corresponding to the mass of methylated species of d-PIM2 (m/z 671.17 [$\text{M}-\text{H}]^-$), and a tetra-mannoside (M4) lacking the GPI anchor (m/z 701.19 [$\text{M} + \text{Cl}]^-$).

digestion released phosphatidyl-*myo*-inositol dimannoside (also known as PIM₂) with m/z 671.1805 [$\text{M}-\text{H}]^-$ instead of m/z 657.1541 [$\text{M}-\text{H}]^-$ confirming that the methylation of *Mabs* LM occurs on its reducing end [Figure 3B]. Since PIM₂ also exist as free glycolipids populating in abundance mycobacterial membranes in the form of monoacylated PIM₂ (Ac₁PIM₂) and diacylated PIM₂ (Ac₂PIM₂), we used PIM₂ for further analyses of the location of the methyl group. PIM₂ were purified from the total lipid extracts from WT *Mabs* and deacylated. In agreement with our analysis of alditol acetates derived from deacylated PIM₂ [Figure 1C], LC/MS analysis of the purified deacylated material revealed a compound with m/z 671.1805 [$\text{M}-\text{H}]^-$ consistent with the methylation of PIM₂

[Figure S1]. Thus, one of the two mannosyl residues on PIM₂ was methylated. To determine which one, purified acylated PIM₂ were next submitted to NMR analysis. The methyl group was clearly observed on the 1D ^1H spectrum of Ac₂PIM₂ in D_2O as a singlet at 3.23 ppm and identified by the correlation between this proton and a carbon at 58.56 ppm on the ^1H – ^{13}C HMQC spectrum [Figure 4]. COSY (not shown) and ^1H – ^{13}C HMQC [Figure 4] data allowed for the assignment of the different spin systems [Table 2], in agreement with previous studies.³⁵ Significant differences between the H2 chemical shifts of both mannose units pointed to the presence of a methyl group on Man1 as its C2 is shifted downfield (79.78 ppm) compared with the Man2 C2 (69.73 ppm). This is

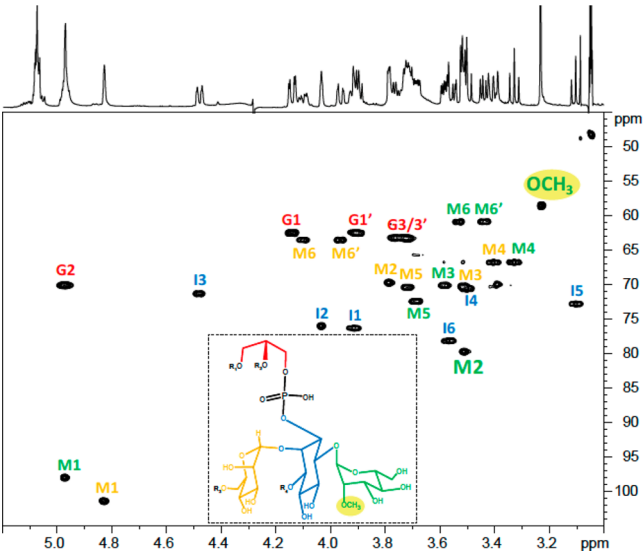


Figure 4. Presence of a methyl group on *Mabs* ATCC 19977 tetra-acylated PIM₂. ¹H–¹³C HMQC spectrum of the tetra-acylated PIM₂ from WT *Mabs* ATCC 19977 in CDCl₃/CD₃OD/D₂O, 60:35:8 (v/v/v) at 298 K. The mannose unit (M) in green is the one located on position 6 of *myo*-Ins (I); the mannose unit in yellow is the one located on position 2 of *myo*-Ins; the Gro unit is symbolized (G). R1–4 correspond to fatty acyl

supported by the observation on the ROESY spectrum of a NOE contact between the methyl group and the Man1 H1 (4.97 ppm) and a correlation between the methyl group and the Man1 C2 (79.78 ppm) on the ¹H–¹³C HMBC spectrum [Figure S2].

Characterization of the Arabinan Domain of *Mabs* LAM. Glycosyl linkage analysis showed that the arabinan portion of LAM possesses the typical linkages found in other mycobacterial LAMs [Table S2] with a number of branches (based on 2-Araf:5-Araf molar ratio) very similar to that reported for *M. smegmatis* LAM.²² Similarly, ¹H–¹³C HMQC spectrum [Figure 2A] and ¹H–¹H TOCSY [Figure 5] highlighted the classical footprints of the different arabinose spin systems previously described:³³ 5-O-Araf (I), 3,5- α -Araf (II), 2-Araf (III), and *t*-Araf (V). LC/MS analysis of the oligoarabinosides released upon *Cellulomonas gelida* endoarabinanase digestion of *Mabs* LAM revealed an equal proportion of linear Ara₄ and branched Ara₆ arabinan termini [Table S4]. In contrast to *M. smegmatis* and *M. tuberculosis* LAM, which harbor phosphoinositol or mannoside caps, respectively, at their nonreducing arabinan termini, further analysis of the *Mabs* digestion products indicated an absence of

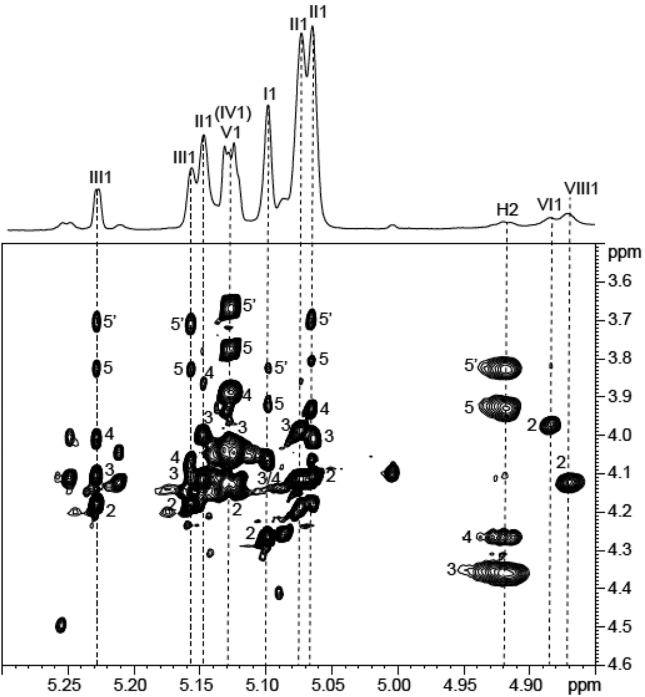


Figure 5. Characterization of the different units of *Mabs* ATCC 19977 LAM by NMR. Expanded region (δ F2 5.30–4.85 and δ F1 3.5–4.6) of the ¹H–¹H TOCSY spectrum of LAM from WT *Mabs* ATCC 19977 dissolved in D₂O at 298 K. I, 3,5 α -Araf; II, 5 α -Araf; III, 2 α -Araf; IV, *t*-Araf; V, β -Araf; VI, 6 α Manp; VII, 3,6 α Manp. Numerals correspond to proton number. The nomenclature used is as described in ref 25. H2 corresponds to the H-2 of the arabinosyl units bearing the succinyl residues.

capping motifs as was reported in *M. chelonae*²⁵ [Figure S3]. This analysis also indicated that the oligoarabinosides released by WT *Mabs* LAM after digestion with *Cellulomonas gelida* endoarabinanase may be modified by a succinyl group and/or an acetyl group with the individual modified oligosaccharides representing 14.5% (succinylated Ara₄), 7.6% (acetylated Ara₄), 0.9% (both modifications) of the total pool of Ara₄, and 5.8% (succinylated Ara₆) and 7.3% (acetylated Ara₆) of the total pool of Ara₆ [Table S4]. Low amounts of succinylated Ara₂ (8.9%) were also detected.

Wild-type LAM was further analyzed for the presence of these succinylated and acetylated residues by 1D and 2D NMR spectroscopy.^{22,25,33} The 1D ¹H spectrum showed the characteristic two pseudotriplets of similar intensities at 2.48 and 2.63 ppm [Figure 6A,B] assigned to methylene groups of succinyl units. Their corresponding carbons were characterized

Table 2. ¹H and ¹³C NMR Chemical Shifts of Tetra-acylated PIM₂ from WT *Mabs* ATCC 19977 Measured at 298 K in CDCl₃/CD₃OD/D₂O, 60:35:8, v/v/v

		1	2	3	4	5	6
Man1 on 6Ins	¹³ C	98.01	79.78	70.12	66.79	72.46	60.90
	¹ H	4.97	3.51	3.59	3.33	3.69	3.44/3.54
Man2 on 2Ins	¹³ C	101.44	69.73	70.34	66.77	70.42	63.55
	¹ H	4.83	3.79	3.51	3.41	3.72	3.97/4.10
<i>myo</i> -Ins	¹³ C	76.33	76.04	71.36	70.61	72.84	78.18
	¹ H	3.92	4.04	4.48	3.49	3.10	3.57
Gro	¹³ C	62.51	70.12	63.29			
	¹ H	3.91/4.14	4.97	3.76/3.72			

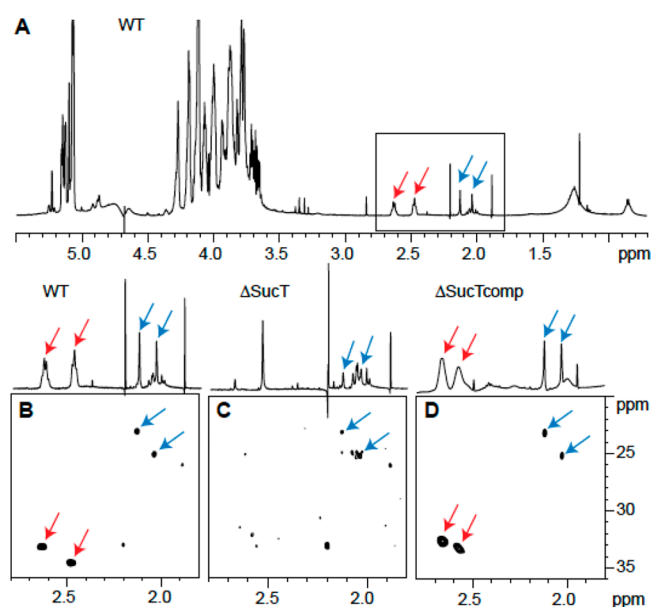


Figure 6. Presence of acetate and succinate residues on WT *Mabs* LAM. NMR analysis of LAM prepared from the WT, mutant (Δ sucT), and complemented mutant (Δ sucT comp) strains. Shown are 1D ^1H (A) and expanded region (δ ^1H 2.80–1.80 and δ ^{13}C 36–20) of the 2D ^1H – ^{13}C (B–D) HMQC NMR spectra. Arrows point to the signals typifying acetates (blue) and succinates (red) (see text for details).

at 34.7 and 33.3 ppm, respectively, on the 2D ^1H – ^{13}C HMQC spectrum [Figure 6B]. Besides these residues, two singlets at 2.13 and 2.04 ppm correlating with two carbons at 23.2 and 25.2 ppm, respectively, define two acetyl groups. All these protons (at 2.48, 2.63, 2.13, and 2.04 ppm) showed a correlation with carbons around 180 ppm typifying carbonyl groups (not shown). The cross-peak between ^1H 4.92/ ^{13}C 82.1 further typifies the presence of succinyl residues on the C2 of -3,5-Araf residues, as described by Delmas et al.³³

In light of the results of our structural analyses, the MABSC LAM structure represented on Figure 7 is proposed.

Disruption of *sucT* in *Mabs*. Given the proposed involvement of the succinyl substituents of *M. tuberculosis* LAM in pathogenicity,²³ we next sought to generate a succinyl-deficient mutant of *Mabs*. A search for orthologs of the SucT succinyltransferase of *M. tuberculosis* (Rv1565c) and *M. smegmatis* (MSMEG_3187) identified one candidate in *Mabs* ATCC 19977. MAB_2689 shares 61% identity (73% similarity) and 58% identity (69% similarity) with its *M. tuberculosis* and *M. smegmatis* counterparts (with a 100% coverage), respectively, and displays the expected secondary structure and conserved cytoplasmic and transmembrane functional amino acid residues of prokaryotic trans-acylases (COG1835) involved in the *O*-acylation of carbohydrates^{40–42} [Figure S4].

MAB_2689 (*sucT*) was disrupted by homologous recombination, yielding *Mabs* Δ sucT [Figure S5]. A complemented mutant strain was generated by expressing in *Mabs* Δ sucT a wild-type (WT) copy of the *Mabs* *sucT* gene from the integrative plasmid pMV306-*sucT*. Preliminary analysis of the lipoglycans from the WT, mutant and complemented mutant strains by SDS-PAGE showed that the migration profile of the mutant LAM was altered [Figure 8], as expected of a form LAM having undergone a change in charge as a result of losing

succinyl residues.²² The migration profile of the mutant LAM reverted back to WT upon complementation with *sucT* expressed from pMV306, but not when the empty pMV306 plasmid was used [Figure 8].

***Mabs* Δ sucT Produces Lipoglycans Structurally Similar to Those of WT *Mabs* except for the Loss of Succinyl Groups on LAM.**

The impact of disrupting *sucT* on the succinylation of LAM was first verified by GC/MS upon butanolysis of LAM prepared from the WT, mutant and complemented mutant strains to yield dibutyl esters of any succinyl groups present.²² This analysis revealed an almost complete absence of succinates in the mutant LAM which were essentially restored in the complemented mutant. Quantitation of succinyl to arabinosyl residues showed a ratio of 1:327 (S.D. \pm 20 for two determinations) for the mutant strain, 1:20 (S.D. \pm 4 for four determinations) for the WT strain, and 1:22.5 (S.D. \pm 1.5 for three determinations) for *Mabs* Δ sucT/pMV306-*sucT* [Figure 9]. The absence of succinates on the mutant LAM was further confirmed by comparative LC/MS analysis of the oligoarabinosides released by the WT, mutant, and complemented mutant LAM upon digestion with *Cellulomonas gelida* endoarabinanase. Whereas oligoarabinosides bearing acetyl substituents were detected in the LAM digestion products from all three strains, succinylated oligoarabinosides were missing from the *Mabs* Δ sucT LAM [Table S4]. Finally, the 1D ^1H and 2D ^1H – ^{13}C HMQC spectra of the mutant LAM [Figure 6C] confirmed the absence of signals typifying the succinyl groups and their restoration upon genetic complementation [Figure 6D], whereas the signals and correlations revealing the acetyl groups remained present in the mutant LAM [Figure 6C].

Quantitative analyses of the alditol acetate and per-*O*-methylated alditol acetate derivatives of the WT, mutant and complemented mutant LAM otherwise did not point to any significant alterations in the Araf to Manp ratio of the mutant LAM [Table S1] or increase in the degree of branching of its mannan and arabinan domains [Table S2]. The relative proportion of Ara₄ to Ara₆ arabinan termini of LAM was also similar in the WT and mutant strains [Table S4] as was the fatty acyl composition of their LM and LAM lipid anchors [Table S3].

***Mabs* Δ sucT Produces an AG Devoid of Succinyl Residues on the Arabinan Domain.**

Given the involvement of SucT from *M. smegmatis* in the succinylation of both LAM and AG,²² we next probed the degree of succinylation of AG in the WT, mutant and complemented mutant strains by subjecting their purified mycolyl-AG-peptidoglycan (mAGP) complex to the same butanolysis procedure as for LAM. The mutant mAGP showed a dramatic decrease in succinate content relative to WT mAGP which was restored to WT levels in the complemented mutant strain [Figure 9]. Quantitation of succinyl to arabinosyl residues yielded a ratio of 1:59 (S.D. \pm 12 for two determinations) for the WT strain, 1:382 (S.D. \pm 4 for two determinations) for *Mabs* Δ sucT, and 1:80 (S.D. \pm 24 for two determinations) for *Mabs* Δ sucT/pMV306-*sucT*. The fact that *Mabs* Δ sucT mAGP was not entirely devoid of succinates as per the butanolysis analysis could indicate that succinyl groups substitute, in a SucT-independent manner, some other positions of AG or of the peptidoglycan or mycolic acid moieties of mAGP.

Analyses of the monosaccharide composition [Table S5] and glycosyl linkages [Table S6] of the WT, mutant and complemented mutant AG otherwise failed to reveal any

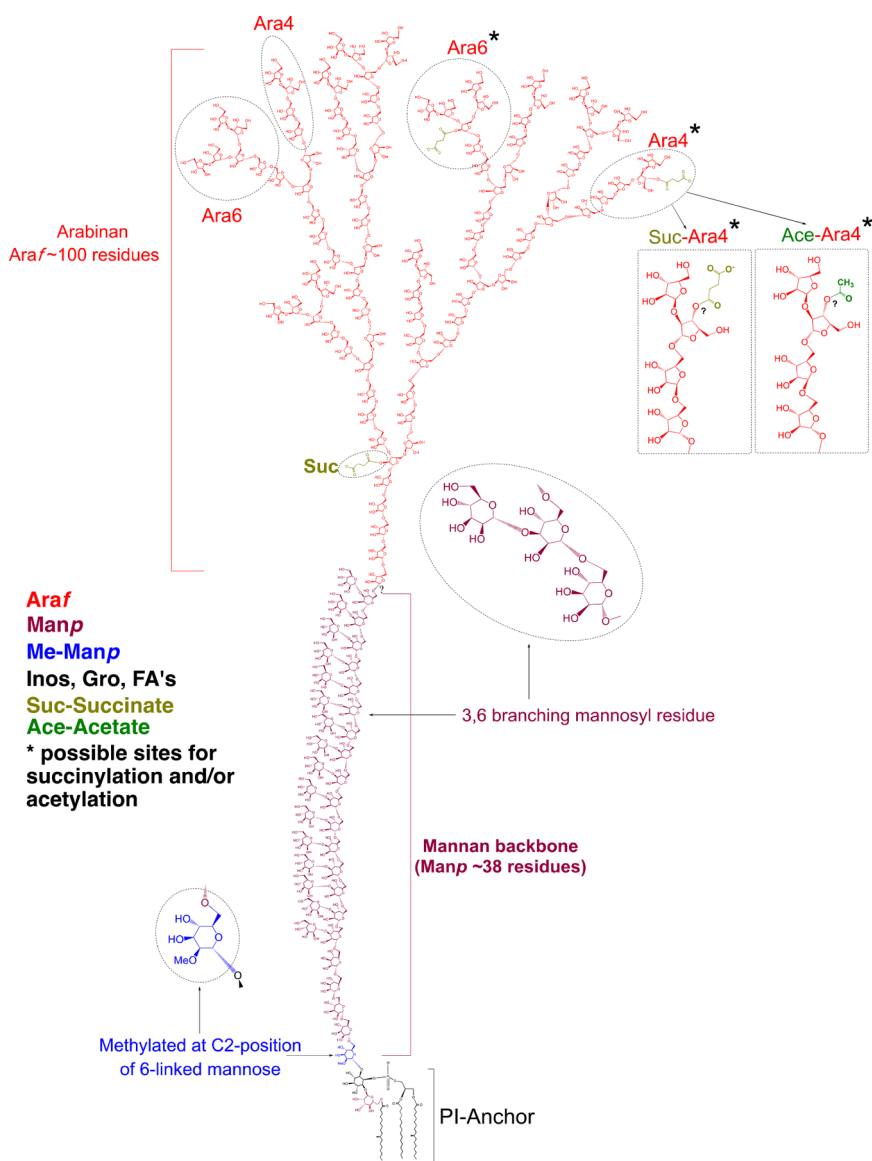


Figure 7. Proposed structure of *Mabs* LAM, consistent with available data. Nonreducing arabinan termini of *Mabs* LAM are devoid of capping residues. The core structure of the arabinan domain consists of ~100 D-Araf residues including linear α -1,5-linked residues and α -1,3 branch points. The arabinan domain is terminated with β -D-Araf-1,2- α -D-Araf at the nonreducing end and there is an equal proportion of linear Ara₄ and branched Ara₆ arabinan termini. Succinyl residues substitute both internal and terminal arabinosyl residues, whereas acetyl residues substitute terminal arabinosyl residues. The precise positions of the succinyl and acetyl residues substituting the terminal arabinosyl residues are currently not known. The mannan backbone with 38 α -D-Manp residues (dominant species per Figure 3A) is composed of linear α -1,6-linked residues and α -3,6 branch points. A single α -1,6-linked Manp residue located at the reducing end of the mannan backbone is methylated at the C-2 position. Further analyses are required to determine the covalent linkage of the arabinan domain to the mannan backbone and the precise structural organization of these two domains. Inos, Inositol; Gro, glycerol; FA, fatty acyl chains.

significant structural alterations in the galactan or arabinan domains of the mutant AG. The degree of mycolylation of the mutant AG was also similar to that measured in the WT and complemented mutant strains [Table S5].

Alterations in the Cell Surface Properties of the *Mabs* *sucT* Mutant. Because *sucT* mutants of *M. marinum*, *M. avium*, and *M. smegmatis* had previously been reported to differ from their WT parent in terms of their cell surface properties reflecting in colony morphology, surface hydrophobicity, biofilm-forming capacity and/or propensity to aggregate in liquid broth,^{22,43,44} we first set out to compare the phenotypes of the *Mabs* WT, mutant and complemented mutant in a panel of in vitro assays.

Monitoring of the absorbance of *Mabs* cultures over time in 7H9-ADC-tyloxapol medium at 37 °C pointed to a slight reduction in growth of the *sucT* knockout in that the mutant never quite reached the same high cell density as the WT and complemented mutant strains did [Figure 10A]. This phenotype was not due to the hyper-aggregation of the mutant cells. Comparable to the situation with the *M. smegmatis* *sucT* knockout mutant,²² we found *Mabs*Δ*sucT* to bind ~3 times more Congo Red than the WT and complemented strains, pointing to an increase in its cell surface hydrophobicity [Figure 10B]. Differences in Congo Red binding also reflected on TS agar supplemented with Congo Red where the WT and complemented mutant strains grew as white colonies whereas *Mabs*Δ*sucT* grew as red colonies [Figure 10B]. Since

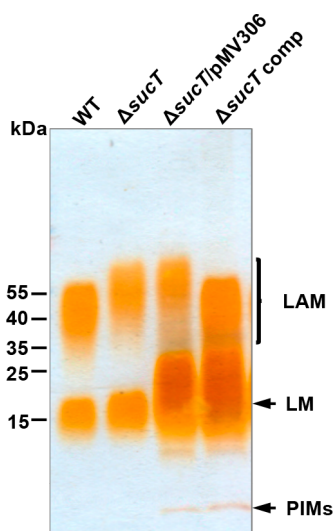


Figure 8. Electrophoretic mobility of lipoglycans from WT *Mabs* ATCC 19977, the *sucT* mutant and the complemented *sucT* mutant. Lipoglycans extracted from WT *Mabs* ATCC 19977, *Mabs*Δ*sucT*, *Mabs*Δ*sucT* harboring an empty pMV306 plasmid, and *Mabs*Δ*sucT*/pMV306-*sucT* (Δ*sucT* comp) were run on a 10–20% Tricine gel followed by periodic acid-silver staining. The results presented are representative of three independent SDS-PAGE runs using different lipoglycan preparations from each strain.

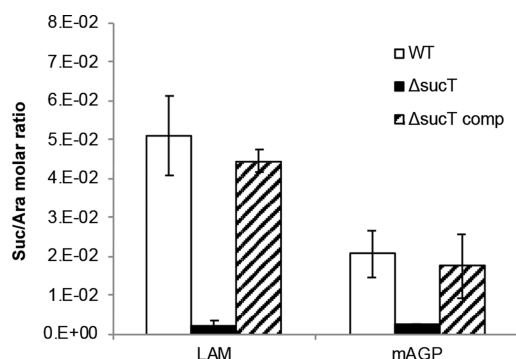


Figure 9. Succinate content of AG and LAM prepared from WT *Mabs* ATCC 19977, the *sucT* mutant, and the complemented mutant strain. Quantification of succinates and arabinose residues in the same LAM and mAGP samples prepared from the WT, mutant, and complemented mutant strains. Results are expressed as average \pm SD succinate/arabino molar ratios from three technical replicates.

Congo Red is known to bind polysaccharides, we verified that this difference in Congo Red binding was not due to the differential binding of the dye to succinylated versus nonsuccinylated LAM in the cells. The results, which are presented in Figure S6, show that Congo Red actually does not bind any variant of the lipoglycan, despite showing evidence of binding to the positive control, carboxymethylcellulose.

Other phenotypic tests essentially yielded negative results. Unlike *M. smegmatis* and *M. avium* *sucT* knockouts,^{22,43} *Mabs*Δ*sucT* displayed a WT colonial morphology on 7H11-OADC agar [Figure S7A]. To our surprise, and in striking contrast with the situation in *M. avium*,⁴³ *Mabs*Δ*sucT* was also as proficient at forming biofilms as its WT parent [Figure S7B]. Under the culture conditions tested therein, the *Mabs* knockout also did not display the hyper-aggregative phenotype characteristic of *M. smegmatis* and *M. marinum* *sucT* mutants.^{22,44} Finally, comparison of the sliding motility of

the WT and mutant strains on 7H9-ADC agar with or without 0.05% Tween-80 did not reveal any obvious differences between strains (data not shown).

Drug susceptibility testing using different classes of antibiotics used in the clinical treatment of NTM infections did not point to any noticeable alterations in the susceptibility of the *sucT* mutant to antibiotics [Table S7]. Finally, because of the negative charge imparted by succinate and acetate on LAM and AG and of the known impact of the charge of LPS and teichoic acids on the susceptibility of Gram-negative and Gram-positive bacteria to cationic antimicrobial peptides,^{45–48} we compared *Mabs*Δ*sucT* to its WT parent for their level of resistance to LL-37 and HNP-1. The MICs of both peptides against the *Mabs* strains tested herein were very high ($>100 \mu\text{g mL}^{-1}$); however, no dramatic increase in the susceptibility of the *sucT* mutant was noted [Table S7].

Impaired Replication and Intracellular Survival of the *Mabs sucT* Mutant in Macrophages and Epithelial Cells.

Since changes in the cell surface hydrophobicity of *Mabs* caused by a deficiency in LAM and/or AG succinylation might have impacted the way the bacterium interacted with host cells, we next proceeded to compare the uptake and intracellular survival of the *Mabs* WT, *sucT* knockout and complemented mutant strain in human monocyte-derived THP-1 macrophages, A549 lung alveolar type II epithelial cells and BEAS-2B bronchial mucosal epithelial cells. A significant reduction in entry of the mutant compared to the WT and complemented mutant were noted in THP-1 macrophages and A549 epithelial cells [Figure 11A,B]. In all cellular models tested, the mutant further showed reduced intracellular survival compared to the WT parent [Figure 11A–C]. Survival in all cell types was restored to WT levels in the complemented mutant. A comparison of the ability of the three *Mabs* strains to translocate across polarized monolayers of human A549 lung alveolar type II epithelial cells, in contrast, failed to reveal any impact of the loss of AG and LAM succinylation [Table S8].

Inhibition of reactive oxygen species by treatment with superoxide dismutase and of phagosome acidification by treatment with bafilomycin A1 both significantly enhanced the ability of *Mabs* WT and complemented mutant strains to replicate inside THP-1 macrophages [Figure S8]. In contrast, the same treatments had a much more modest effect on the intracellular replication and persistence of *Mabs*Δ*sucT* indicating that a combination of factors most likely accounts for the reduced ability of the knockout mutant to survive inside macrophages.

DISCUSSION

The studies described therein reveal for the first time the structures of *Mabs* PIM, LM, and LAM [Figure 7] and support polysaccharides as key cell envelope constituents modulating the virulence of MABSC.

In common with the closely related species, *M. chelonae*, *Mabs* LAM is devoid of capping motifs at the nonreducing arabinan termini, and the mannan domain of both LM and LAM harbors α -1,3-Manp side chains instead of the α -1,2-Manp side chains normally found in *M. smegmatis* and *M. tuberculosis*. The size of the mannan domain of *Mabs* LM (33–44 mannosyl residues) is considerably larger than that of *M. smegmatis* (23–29 mannosyl residues). As has been reported in *M. tuberculosis*, *M. smegmatis* and a number of other tuberculous and nontuberculous mycobacteria,^{22,23,28,33,34,49} succinyl substituents modify the LAM and

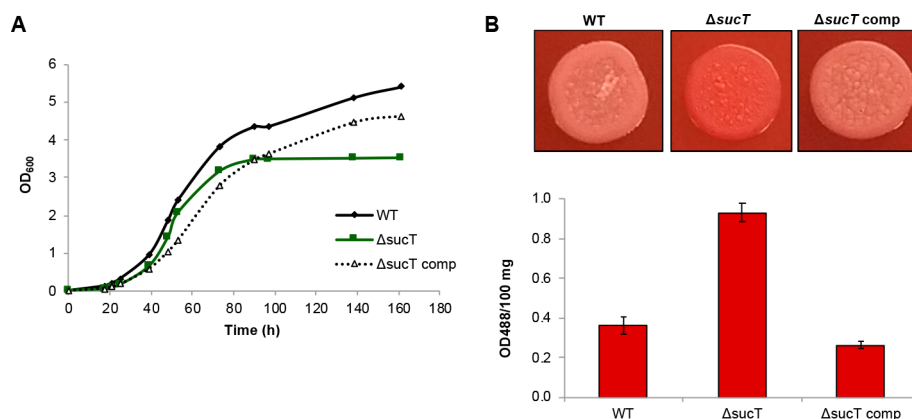


Figure 10. Growth characteristics and cell envelope properties of the *Mabs* *sucT* mutant. (A) Growth characteristics of WT *Mabs* ATCC 19977, the *sucT* mutant and the complemented mutant strain in 7H9-ADC-Tween 80 at 37 °C. The results presented are representative of three independent experiments. (B) Congo Red binding on TS agar plate (top panel) and in TS liquid medium (graph). Shown on the graph are the average \pm SD absorbances of acetone extracts measured for three biological replicates.

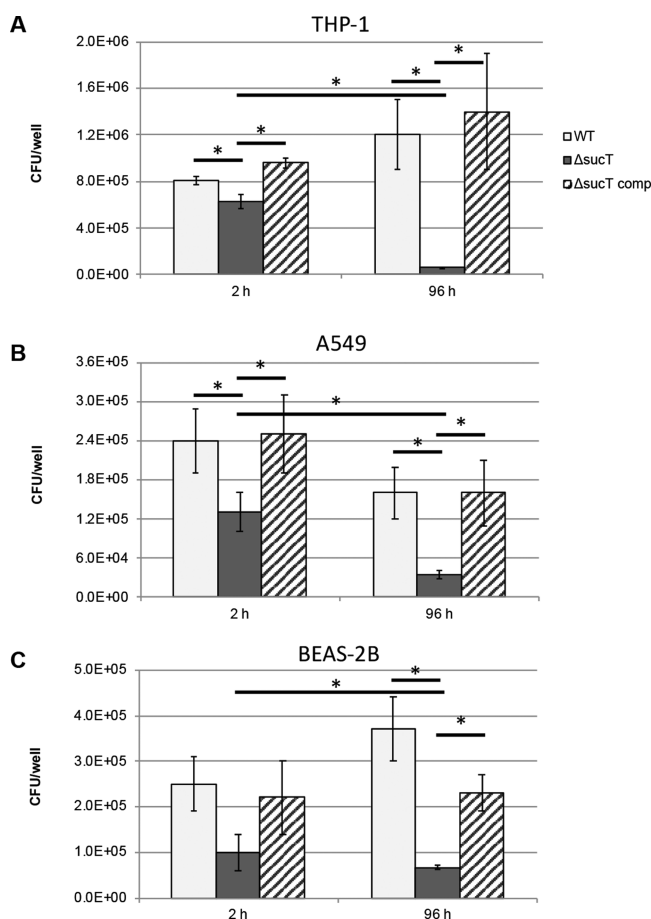


Figure 11. Invasion and intracellular replication of *Mabs* WT, mutant and complemented mutant strains in (A) THP-1 macrophages, (B) A549 lung alveolar type II epithelial cells, and (C) BEAS-2B bronchial mucosal epithelial cells. Cells were infected at a MOI of 10 bacteria per cell and intracellular CFUs counted after 2 and 96 h of infection. Data is shown as mean values \pm SD of triplicate wells. Statistical analysis using 2-way ANOVA, * p < 0.05. The results presented are representative of three independent experiments.

AG of *Mabs*. While their position on AG was not precisely determined in this study, we were able to map these modifications to the C2 of α -3,5-Araf residues and other as

yet incompletely defined positions of the arabinan termini of LAM. We further identified the succinyltransferase encoded by *MAB_2689* (*sucT*) as the sole enzyme responsible for their addition onto the lipoglycan. Most strikingly and unique among all mycobacterial LMs and LAMs whose structures have been reported to date, is the presence of acetyl substituents modifying the arabinan termini of LAM and the finding of a methylated mannopyranosyl residue linked to position 6 of the *myo*-inositol residue of PIM, LM and LAM.

In *M. tuberculosis*, the transfer of a Manp to position 6 of the *myo*-inositol residue of PIM is mediated by the GDP-Manp-dependent mannosyltransferase PimB'.⁵⁰ In line with the methylation of this Manp residue in *Mabs* but not in any other mycobacteria analyzed to date, we note that *Mabs* *pimB'* (*MAB_1976*) maps in the genome of *Mabs* ATCC 19977 right upstream a gene annotated as a putative S-adenosyl-methionine-dependent methyltransferase (*MAB_1977*). Only nine base-pairs separate the stop codon of *pimB'* from the start codon of *MAB_1977* indicating that the two genes may be cotranscribed. Orthologs of *MAB_1977* were found in the genomes of a few NTM species including *M. immunogenum*, *M. chelonae*, and *M. talmoniae*, as well as in some *Nocardia*, but were noticeably absent from *M. tuberculosis*, *M. avium*, *M. smegmatis*, and *M. leprae*.

The modification of LPS with discrete covalent substituents such as acyl chains, phosphates, aminosugars, phosphoethanolamine and methyl groups is a well-established strategy used by Gram-negative bacteria to promote adaptation and survival under various stress conditions. For instance, another pathogen of the CF lung, *Pseudomonas aeruginosa*, has been reported to modify the lipid A and O-antigen moieties of LPS with acyl groups, aminosugars and methyl substituents to modulate acute versus chronic infection and evade detection by the host.^{47,51} Much less is known of the biological significance of the discrete covalent substituents found on mycobacterial LAM⁵² despite indications that succinyl residues may become more prevalent on *M. tuberculosis* LAM during host infection.²³ To gain insight into the biological significance of succinyl substituents, a *sucT* knockout mutant of *Mabs* ATCC 19977 was constructed and submitted to a panel of biochemical analyses and phenotypic assays in vitro and ex vivo. In line with previous observations made on a *M. smegmatis* *sucT* mutant,²² succinylation of AG and LAM in *Mabs* had no apparent impact

on the biosynthesis of these polysaccharides, or on the mycolylation of AG. These findings contrast with the report of a *M. marinum* *sucT* mutant in which various aspects of LAM biosynthesis were found to be impaired, including mannoside capping, acylation of the phosphatidylinositol mannoside anchor, and branching of the mannan and arabinan domains.²³ On the basis of these observations, it thus seems unlikely that succinyl substituents act as conserved molecular signals governing the biosynthesis of AG and LAM in slow and fast-growing mycobacteria. A common trait of all mycobacterial *sucT* mutants generated to date, however, relates to their altered surface properties reflecting in one or more of the following phenotypes: Changes in colony morphology (*M. avium* and *M. smegmatis*),^{22,43} reduced biofilm forming capacity (*M. avium*),⁴⁴ hyper-aggregation (*M. smegmatis* and *M. marinum*),^{22,44} and increased surface hydrophobicity (*M. smegmatis*, *Mabs*) and rigidity (*M. smegmatis*).²² It is thus reasonable to propose that the succinylation of the two major cell envelope polysaccharides of mycobacteria serves to modulate—most likely through indirect, charge-mediated, effects—the cell surface properties of the bacilli. Because the composition of the cell envelope varies across *Mycobacterium* species, as does the structure of LAM that bears some of these substituents, it is to be expected that the qualitative and quantitative impact of succinylation will be species-dependent. The different effects associated with AG and LAM succinylation on the interactions of *Mabs* and *M. avium* with host cells further supports this assumption. Whereas a *M. avium* *sucT* mutant was significantly impaired in its ability to invade BEAS-2B human bronchiolar epithelial cells²¹ while displaying no apparent uptake or replication phenotype in THP-1 macrophages,⁵³ the corresponding *Mabs* mutant was not as dramatically impaired in BEAS-2B invasion but displayed reduced uptake by both THP-1 macrophages and A549 epithelial cells, and much reduced intracellular survival in all cell types analyzed in this study. Clearly, while conserved in slow- and fast-growing, pathogenic and nonpathogenic *Mycobacterium* species, the biological significance of polysaccharide succinylation in mycobacteria is contextual and more studies will be required to decipher their physiological and pathogenic impact as well as the underlying molecular mechanisms. Apparently more restricted in distribution across mycobacteria are the acetyl and methyl substituents of PIM, LM and LAM. The acetates bring additional negative charges to those conferred by the succinates to specific regions of the arabinan domain of LAM and may play a similar role in modulating the interactions of MABSC with host cells. The methylation of PIM and of the lipid anchor of LM and LAM, on the other hand, somewhat increases the hydrophobicity of these molecules and may impact the integrity and the permeability of the inner and outer membranes in which they are anchored.

METHODS

Bacterial Strains and Growth Conditions. *Mabs* ATCC 19977 was grown under agitation at 37 °C in Middlebrook 7H9 medium supplemented with 10% albumin-dextrose-catalase (ADC) (BD Sciences) and 0.05% Tween 80, in cation-adjusted Mueller Hinton II broth (BD Sciences) with 0.05% tyloxapol, in Tryptic Soy (TS) broth with 0.05% tyloxapol, or on Middlebrook 7H11 agar supplemented with 10% oleic acid-albumin-dextrose-catalase (OADC) (BD

Sciences). Zeocin (Zeo) and kanamycin (Kan) were added to the culture media at a final concentration of 100 $\mu\text{g mL}^{-1}$.

***Mabs sucT* Knockout Mutant.** Recombineering was used to inactivate the *sucT* (MAB_2689) gene of *Mabs* ATCC 19977 by allelic replacement. To this end, the Gp60 and Gp61 recombineering proteins from mycobacteriophage Che9c were expressed from the replicative plasmid pJV53-XylE under control of an acetamide-inducible promoter.^{54,55} Acetamide-induced *Mabs* ATCC 19977 harboring pJV53-XylE were electrotransformed with ~500 ng of linear allelic exchange substrate consisting of the Zeo resistance cassette bracketed by ~500 bp of upstream and downstream homologous DNA sequence flanking *sucT*. Double crossover candidates were selected on Zeo-containing plates and confirmed by PCR. For complementation, the entire coding sequence of *Mabs sucT* was PCR-amplified from *Mabs* ATCC 19977 genomic DNA and cloned into the integrative plasmid pMV306, yielding pMV306-*sucT*. Primer sequences for all constructs are available upon request.

Preparation of Lipids, Lipoglycans, and Arabinogalactan. Extraction of total lipids, lipoglycans, and the mycolyl-AG-peptidoglycan (mAGP) complex from *Mabs* cells followed procedures described earlier for the characterization of the *M. smegmatis* *sucT* mutant.²² Lipoglycans were purified by gel exclusion chromatography⁵⁶ and analyzed by SDS-PAGE on commercial Novex 10–20% Tricine gels stained with periodic acid Schiff reagent. Polar lipids from WT *Mabs* ATCC 19977 were precipitated from the total lipid extract with acetone at 4 °C overnight, and PIM₂ were further purified from the precipitate by chromatography on a silicic acid column (1.5 × 20 cm) (KG60, 230–400 mesh, Supelco) as described previously.⁵⁷ Purified PIM₂ were dried and deacylated using a 33% methylamine solution in ethanol:water:water saturated butanol (69:23:8) at room temperature overnight (modified protocol from ref 58).

Analytical Procedures. Structural analyses of PIMs, lipoglycans and mAGP followed earlier procedures.²² Briefly, 1 mg of mAGP, 20 μg of acylated PIM₂ and 50 μg of LAM were used for permethylation and alditol acetates preparation and analyzed by GC/MS to determine monosaccharide composition and glycosyl linkage patterns. Digestion of LM with endo- α -(1→6)-D-mannanase from *Bacillus circulans* and analysis of the products of the reaction by LC/MS followed the procedure recently described by Angala et al.³⁸ Succinates were analyzed and quantified by GC/MS analysis as their butyl succinate derivatives obtained from either 20 μg of purified LAM or 1 mg of mAGP. The presence of potential capping motifs at the nonreducing arabinan termini of LAM from *Mabs* was analyzed by LC/MS after digestion of LAM with *Cellulomonas gelida* endoarabinanase. Deacylated PIM₂ and the endoarabinanase digestion products of LAM were directly analyzed by ultraperformance liquid chromatography (UPLC) on an Atlantis T3 column (Waters) using Waters Acquity UPLC H-Class system coupled to a Bruker MaXis Plus QTOF MS instrument according to the method described by De et al.²³

The fatty acids esterifying the mannosylated phosphatidylmyo-inositol anchor of LM and LAM were analyzed as their fatty acid methyl esters (FAME) by GC/MS. Briefly, 100 μg of LM and LAM were methanolized in 100 μL of 3 M methanolic HCl by heating at 80 °C overnight and extracted with *n*-hexane:water (1:1). FAMEs were analyzed on a Thermo Scientific TRACE 1310 Gas Chromatograph paired

with a Thermo Scientific TSQ 8000 Evo Triple Quadrupole GC-MS/MS. Samples were run on a 30 m \times 0.25 mm \times 0.25 μ m Zebron ZB-SHT Inferno capillary column (Phenomenex) at an initial temperature of 60 °C. The temperature was increased to 375 °C at a ramp rate of 20 °C min⁻¹ and held for 5 min. Data handling was carried out using the Thermo Scientific Chromeleon Chromatography Data System software.

Mycolic acids released from mAGP by treatment with 2 M trifluoroacetic acid were quantified by LC/MS as described earlier⁵⁹ on an Agilent 1260 Infinity chromatograph equipped with a 2.1 mm \times 150 mm (3.5 μ m particle size) XBridge reverse phase C18 column (Waters) coupled to an Agilent 6224 time-of-flight (TOF) mass spectrometer. Data were analyzed using the Agilent MassHunter software.

NMR experiments were performed at 298 K with a cryo-probed Bruker DRX600 spectrometer (Karlsruhe, Germany) and a Prodigy cryo-probed Bruker Avance-IV 400 MHz NEO spectrometer for the 2D ¹H–¹³P HMQC sequences. Native molecules were dissolved in D₂O (LM and LAM) or CDCl₃/CD₃OD/D₂O 60/35/8 (PIM) and analyzed in 200 \times 5 mm 535-PP NMR tubes. Proton and carbon chemical shifts are expressed in ppm downfield from the signal of external acetone (δ H 2.22 and δ C 30.89) and those of Ac₂PIM₂ are expressed in ppm downfield from the signal of chloroform (δ H 7.26 and δ C 77.36).

Congo Red Binding and Sliding Motility. *M. smegmatis* strains were tested for Congo Red binding in TS broth and TS agar as described by Etienne et al.⁶⁰ For testing the ability of LAM to bind Congo Red, 5 μ g of LAM from *Mabs* WT and *Mabs*Δ*sucT*, and 5 μ g of carboxymethylcellulose (low viscosity, Sigma) were dot-blotted on a nitrocellulose membrane and either stained with Congo Red (1 mg mL⁻¹ Congo Red solution in 0.1 mol L⁻¹ acetate buffer (pH 3.3)) or immunodetected with CS-35 antibodies. Congo Red staining was performed for 45 min at room temperature with subsequent destaining in water for 30 min at room temperature. For sliding motility assays, *Mabs* strains were drop-inoculated from liquid cultures diluted to 10⁶ CFU mL⁻¹ onto 7H9-ADC medium containing 0.34% agar with or without 0.05% Tween 80 and incubated at 37 °C for 5 days.

Biofilm Assay. Static biofilms were formed in Hanks' balanced salt solution (HBSS) or 7H9-OADC as previously described⁶¹ with minor modifications. Briefly, bacteria were taken from 7H10-OADC agar plates and resuspended in either HBSS or 7H9-OADC to generate a bacterial suspension of \sim 10⁷ CFU mL⁻¹. 150 μ L of this suspension was seeded in 96-well polystyrene (BD, Franklin Lakes, NJ), and the biofilms were allowed to establish for 10 days in the dark at 25 °C. Biofilm biomass was determined by plating and counting CFUs.

Drug Susceptibility Testing. MIC values were determined in cation-adjusted Mueller–Hinton II broth in a total volume of 100 μ L in 96-well microtiter plates. *Mabs* cultures grown to early log phase were diluted to a final concentration of 10⁶ CFU mL⁻¹ and incubated in the presence of serial dilutions of the drugs for 4 days at 37 °C. MICs were determined using the resazurin blue test.⁶²

Macrophage Infection and Survival Assays. Human monocyte THP-1 cells (ATCC) were cultured in suspension in RPMI-1640 (Corning) supplemented with 10% fetal bovine serum (FBS, Gemini) at 37 °C with 5% CO₂. Cells were counted with a hemocytometer, seeded at 80% confluency into 24-well plates and supplemented with 20 ng mL⁻¹ phorbol 12-

myristate 13-acetate (PMA, Sigma-Aldrich) to trigger differentiation into adherent macrophages. After 24 h, the culture medium was replaced and cells were allowed to rest for an additional 24 h prior to infection. THP-1 cells were infected with well-dispersed suspensions of the WT, mutant and complemented mutant strains in PBS at a multiplicity of infection of 10 bacteria per cell for 1 h at 37 °C in a 5% CO₂ atmosphere. Infected cells were then gently washed twice with HBSS, and added fresh culture medium supplemented with 100 μ g mL⁻¹ amikacin (Sigma) for 2 h to kill extracellular bacteria. In some experiments, the culture medium was supplemented with 50 μ g mL⁻¹ superoxide dismutase or 13 nM baflomycin A1 to inhibit reactive oxygen species and vacuolar acidification, respectively. Upon two washes with HBSS, the wells were lysed 2 h, 2 days and 4 days postinfection with 0.1% Triton X-100 for 10 to 15 min and the cell lysates were serially diluted in PBS and plated onto Middlebrook 7H10-OADC agar to count CFUs. Colonies were counted after 5 days of incubation at 37 °C. A modified Trypan blue test was used to monitor the integrity of the monolayer throughout the infection.

Infection of Lung Epithelial Cells. A549 lung alveolar type II epithelial cell line (ATCC) was cultured in DMEM (Corning) supplemented with 10% FBS at 37 °C with 5% CO₂. Human BEAS-2B bronchial mucosal epithelial cells (CRL-9609) were cultured as described in ref 21 in BEBM medium supplemented with BEGM, which contains bovine pituitary extract (BPE), hydrocortisone, human epidermal growth factor (hEGF), epinephrine, transferrin, insulin, retinoic acid, and triiodothyronine (Lonza, Allendale, NJ). Cell infections with *Mabs* were as described for the THP-1 cells except that the infection was synchronized by centrifugation for 5 min at 232g after addition of the bacteria. Killing of extracellular bacteria, cell lysis and CFU counting were as described for THP-1 cells.

Polarized Cell Layer Translocation Assay. A549 epithelial cells grown in DMEM supplemented with 5% FBS were seeded at 2 \times 10⁵ cells per well on the 6.5 mm porous filter membrane of a transwell insert (Corning, Tewksbury, MA). Polarized monolayer achieved confluence after 5 days at 37 °C in a 5% CO₂ atmosphere. Trans-epithelial resistance was measured using a Millicell-ESR apparatus (Millipore) as per the manufacturer's instructions, right at the beginning and at the end of the infection. Final values were obtained by subtracting the blank value, and the results are expressed as ohms/cm². A modified Trypan blue test was also used to monitor the integrity of the monolayer. To determine bacterial translocation through the monolayer, dispersed bacteria were placed in the upper chamber (at a MOI of 10) and the supernatant of the basal chamber was plated after 24 h of infection on 7H10-OADC agar for CFU enumeration.

■ ASSOCIATED CONTENT

Supporting Information

The Supporting Information is available free of charge at <https://pubs.acs.org/doi/10.1021/acsinfectdis.0c00361>.

Structural analysis of PIM and LAM, MIC determinations, comparative analysis of the ability of the wild-type and mutant strains to form biofilms in vitro and translocate across polarized monolayers of human A549 lung alveolar type II epithelial cells, protein sequence analysis, evidence of gene disruption at the *sucT* locus of

Mabs ATCC 19977, colony morphology, and intracellular survival of recombinant strains (PDF)

AUTHOR INFORMATION

Corresponding Author

Mary Jackson – Mycobacteria Research Laboratories,
Department of Microbiology, Immunology, and Pathology,
Colorado State University, Fort Collins, Colorado 80523-1682,
United States; orcid.org/0000-0002-9212-0258;
Email: mary.jackson@colostate.edu

Authors

Zuzana Palčková – Mycobacteria Research Laboratories,
Department of Microbiology, Immunology, and Pathology,
Colorado State University, Fort Collins, Colorado 80523-1682,
United States

Martine Gilleron – Institut de Pharmacologie et de Biologie
Structurale, IPBS, Université de Toulouse, CNRS, UPS, 31077
Toulouse, France

Shiva Kumar Angala – Mycobacteria Research Laboratories,
Department of Microbiology, Immunology, and Pathology,
Colorado State University, Fort Collins, Colorado 80523-1682,
United States

Juan Manuel Belardinelli – Mycobacteria Research
Laboratories, Department of Microbiology, Immunology, and
Pathology, Colorado State University, Fort Collins, Colorado
80523-1682, United States

Michael McNeil – Mycobacteria Research Laboratories,
Department of Microbiology, Immunology, and Pathology,
Colorado State University, Fort Collins, Colorado 80523-1682,
United States

Luiz E. Bermudez – Department of Biomedical Sciences, College
of Veterinary Medicine and Department of Microbiology,
College of Science, Oregon State University, Corvallis, Oregon
97331, United States

Complete contact information is available at:

<https://pubs.acs.org/10.1021/acsinfecdis.0c00361>

Author Contributions

ZP, SKA, MG, JMB, MM, LEB, and MJ designed research. ZP, MG, SKA, JMB, and LEB performed research. ZP, MG, SKA, JMB, MM, LEB, and MJ analyzed data. ZP, MG, SKA, JMB, MM, LEB, and MJ wrote the main manuscript text. All authors reviewed the final version of the manuscript.

Notes

The authors declare no competing financial interest.

ACKNOWLEDGMENTS

This work was supported by the National Institute of Allergy and Infectious Diseases/National Institutes of Health grant AI064798 (to MJ), and an award from the Cystic Fibrosis Foundation (to MJ). The content is solely the responsibility of the authors and does not necessarily represent the official views of the NIH or the Cystic Fibrosis Foundation. We thank the Integrated Screening Platform of Toulouse (PICT, IBISA) for providing access to 600 MHz equipment, Dr. John Spencer (Colorado State University) for the provision of CS-35 antibodies, and Dr. Delphi Chatterjee and Anita Amin (Colorado State University) for the provision of *Cellulomonas gelida* endoarabinanase.

REFERENCES

- (1) Prevots, D. R., and Marras, T. K. (2015) Epidemiology of human pulmonary infection with nontuberculous mycobacteria: a review. *Clin Chest Med.* 36, 13–34.
- (2) Park, I. K., and Olivier, K. N. (2015) Nontuberculous mycobacteria in cystic fibrosis and non-cystic fibrosis bronchiectasis. *Semin Respir Crit Care Med.* 36, 217–224.
- (3) Martiniano, S. L., Nick, J. A., and Daley, C. L. (2019) Nontuberculous Mycobacterial Infections in Cystic Fibrosis. *Thorac Surg Clin* 29, 95–108.
- (4) Bryant, J. M., Grogono, D. M., Rodriguez-Rincon, D., Everall, I., Brown, K. P., Moreno, P., Verma, D., Hill, E., Drijkoningen, J., Gilligan, P., Esther, C. R., Noone, P. G., Giddings, O., Bell, S. C., Thomson, R., Wainwright, C. E., Coulter, C., Pandey, S., Wood, M. E., Stockwell, R. E., Ramsay, K. A., Sherrard, L. J., Kidd, T. J., Jabbour, N., Johnson, G. R., Knibbs, L. D., Morawska, L., Sly, P. D., Jones, A., Bilton, D., Laurensen, I., Ruddy, M., Bourke, S., Bowler, I. C., Chapman, S. J., Clayton, A., Cullen, M., Dempsey, O., Denton, M., Desai, M., Drew, R. J., Edenborough, F., Evans, J., Folb, J., Daniels, T., Humphrey, H., Isalska, B., Jensen-Fangel, S., Jonsson, B., Jones, A. M., Katzenstein, T. L., Lillebaek, T., MacGregor, G., Mayell, S., Millar, M., Modha, D., Nash, E. F., O'Brien, C., O'Brien, D., Ohri, C., Pao, C. S., Peckham, D., Perrin, F., Perry, A., Pressler, T., Prtak, L., Qvist, T., Robb, A., Rodgers, H., Schaffer, K., Shafi, N., van Ingen, J., Walshaw, M., Watson, D., West, N., Whitehouse, J., Haworth, C. S., Harris, S. R., Ordway, D., Parkhill, J., and Floto, R. A. (2016) Emergence and spread of a human-transmissible multidrug-resistant nontuberculous mycobacterium. *Science* 354, 751–757.
- (5) Wu, M. L., Aziz, D. B., Dartois, V., and Dick, T. (2018) NTM drug discovery: status, gaps and the way forward. *Drug Discovery Today* 23, 1502–1519.
- (6) Daffé, M., and Draper, P. (1997) The envelope layers of mycobacteria with reference to their pathogenicity. *Adv. Microb. Physiol.* 39, 131–203.
- (7) Jackson, M. (2014) The Mycobacterial Cell Envelope-Lipids. *Cold Spring Harbor Perspect. Med.* 4, No. a021105.
- (8) Howard, S. T., Rhoades, E., Recht, J., Pang, X., Alsop, A., Kolter, R., Lyons, C. R., and Byrd, T. F. (2006) Spontaneous reversion of *Mycobacterium abscessus* from a smooth to a rough morphotype is associated with reduced expression of glycopeptidolipid and reacquisition of an invasive phenotype. *Microbiology* 152, 1581–1590.
- (9) Nessar, R., Reyat, J. M., Davidson, L. B., and Byrd, T. F. (2011) Deletion of the mmpL4b gene in the Mycobacterium abscessus glycopeptidolipid biosynthetic pathway results in loss of surface colonization capability, but enhanced ability to replicate in human macrophages and stimulate their innate immune response. *Microbiology* 157, 1187–1195.
- (10) Jonsson, B., Ridell, M., and Wold, A. E. (2013) Phagocytosis and cytokine response to rough and smooth colony variants of Mycobacterium abscessus by human peripheral blood mononuclear cells. *APMIS* 121, 45–55.
- (11) Bernut, A., Herrmann, J. L., Kissa, K., Dubremetz, J. F., Gaillard, J. L., Lutfalla, G., and Kremer, L. (2014) Mycobacterium abscessus cording prevents phagocytosis and promotes abscess formation. *Proc. Natl. Acad. Sci. U. S. A.* 111, E943–E952.
- (12) Roux, A. L., Viljoen, A., Bah, A., Simeone, R., Bernut, A., Laencina, L., Deramaut, T., Rottman, M., Gaillard, J. L., Majlessi, L., Brosch, R., Girard-Misguich, F., Vergne, I., de Chastellier, C., Kremer, L., and Herrmann, J. L. (2016) The distinct fate of smooth and rough Mycobacterium abscessus variants inside macrophages. *Open Biol.* 6, 160185.
- (13) Whang, J., Back, Y. W., Lee, K. I., Fujiwara, N., Paik, S., Choi, C. H., Park, J. K., and Kim, H. J. (2017) Mycobacterium abscessus glycopeptidolipids inhibit macrophage apoptosis and bacterial spreading by targeting mitochondrial cyclophilin D. *Cell Death Dis.* 8, No. e3012.
- (14) Malcolm, K. C., Caceres, S. M., Pohl, K., Poch, K. R., Bernut, A., Kremer, L., Bratton, D. L., Herrmann, J. L., and Nick, J. A. (2018)

Neutrophil killing of *Mycobacterium abscessus* by intra- and extracellular mechanisms. *PLoS One* 13, No. e0196120.

(15) Llorens-Fons, M., Perez-Trujillo, M., Julian, E., Brambilla, C., Alcaide, F., Byrd, T. F., and Luquin, M. (2017) Trehalose Polyphosphates, External Cell Wall Lipids in *Mycobacterium abscessus*, Are Associated with the Formation of Clumps with Cording Morphology, Which Have Been Associated with Virulence. *Front. Microbiol.* 8, 1402.

(16) Laencina, L., Dubois, V., Le Moigne, V., Viljoen, A., Majlessi, L., Pritchard, J., Bernut, A., Piel, L., Roux, A. L., Gaillard, J. L., Lombard, B., Loew, D., Rubin, E. J., Brosch, R., Kremer, L., Herrmann, J. L., and Girard-Misguich, F. (2018) Identification of genes required for *Mycobacterium abscessus* growth in vivo with a prominent role of the ESX-4 locus. *Proc. Natl. Acad. Sci. U. S. A.* 115, E1002–E1011.

(17) Dubois, V., Viljoen, A., Laencina, L., Le Moigne, V., Bernut, A., Dubar, F., Blaise, M., Gaillard, J. L., Guerardel, Y., Kremer, L., Herrmann, J. L., and Girard-Misguich, F. (2018) MmpL8MAB controls *Mycobacterium abscessus* virulence and production of a previously unknown glycolipid family. *Proc. Natl. Acad. Sci. U. S. A.* 115, E10147–E10156.

(18) Mishra, A. K., Driessen, N. N., Appelmelk, B. J., and Besra, G. S. (2011) Lipoarabinomannan and related glycoconjugates: structure, biogenesis and role in *Mycobacterium tuberculosis* physiology and host-pathogen interaction. *FEMS Microbiol. Rev.* 35, 1126–1157.

(19) Vergne, I., Gilleron, M., and Nigou, J. (2015) Manipulation of the endocytic pathway and phagocyte functions by *Mycobacterium tuberculosis* lipoarabinomannan. *Front. Cell. Infect. Microbiol.* 4, 187.

(20) Turner, J., and Torrelles, J. B. (2018) Mannose-capped lipoarabinomannan in *Mycobacterium tuberculosis* pathogenesis. *Pathog. Dis.*, DOI: 10.1093/femspd/fty026.

(21) Yamazaki, Y., Danelishvili, L., Wu, M., Hidaka, E., Katsuyama, T., Stang, B., Petrofsky, M., Bildfell, R., and Bermudez, L. E. (2006) The ability to form biofilm influences *Mycobacterium avium* invasion and translocation of bronchial epithelial cells. *Cell. Microbiol.* 8, 806–814.

(22) Palcekova, Z., Angala, S. K., Belardinelli, J. M., Eskandarian, H. A., Joe, M., Brunton, R., Rithner, C., Jones, V., Nigou, J., Lowary, T. L., Gilleron, M., McNeil, M., and Jackson, M. (2019) Disruption of the SucT acyltransferase in *Mycobacterium smegmatis* abrogates succinylation of cell envelope polysaccharides. *J. Biol. Chem.* 294, 10325–10335.

(23) De, P., Shi, L., Boot, C., Ordway, D., McNeil, M., and Chatterjee, D. (2020) Comparative Structural Study of Terminal Ends of Lipoarabinomannan from Mice Infected Lung Tissues and Urine of a Tuberculosis Positive Patient. *ACS Infect. Dis.* 6, 291–301.

(24) Pitarque, S., Larrouy-Maumus, G., Payré, B., Jackson, M., Puzo, G., and Nigou, J. (2008) The immunomodulatory lipoglycans, lipoarabinomannan and lipomannan, are exposed at the mycobacterial cell surface. *Tuberculosis* 88, 560–565.

(25) Guérardel, Y., Maes, E., Ellass, E., Leroy, Y., Timmerman, P., Besra, G. S., Lochter, C., Strecker, G., and Kremer, L. (2002) Structural study of lipomannan and lipoarabinomannan from *Mycobacterium chelonae*. *J. Biol. Chem.* 277, 30635–30648.

(26) Kaur, D., Angala, S. K., Wu, S. W., Khoo, K. H., Chatterjee, D., Brennan, P. J., Jackson, M., and McNeil, M. R. (2014) A single arabinan chain is attached to the phosphatidylinositol mannosyl core of the major immunomodulatory mycobacterial cell envelope glycoconjugate, lipoarabinomannan. *J. Biol. Chem.* 289, 30249–30256.

(27) Shi, L., Berg, S., Lee, A., Spencer, J. S., Zhang, J., Vissa, V., McNeil, M. R., Khoo, K.-H., and Chatterjee, C. (2006) The carboxy terminus of EmbC from *Mycobacterium smegmatis* mediates chain length extension of the arabinan in lipoarabinomannan. *J. Biol. Chem.* 281, 19512–19526.

(28) Bhamidi, S., Scherman, M. S., Rithner, C. D., Prenni, J. E., Chatterjee, D., Khoo, K.-H., and McNeil, M. R. (2008) The identification and location of succinyl residues and the characterization of the interior arabinan region allows for a model of the

complete primary structure of *Mycobacterium tuberculosis* mycolyl arabinogalactan. *J. Biol. Chem.* 283, 12992–13000.

(29) Gilleron, M., Jackson, M., Nigou, J., and Puzo, G. (2008) Structure, activities and biosynthesis of the Phosphatidyl-myoinositol-based lipoglycans. In *The Mycobacterial Cell Envelope* (Daffé, M., and Reyrat, J.-M. eds.), pp 75–105, ASM Press, Washington, DC.

(30) Angala, S. K., Belardinelli, J. M., Huc-Claustre, E., Wheat, W. H., and Jackson, M. (2014) The cell envelope glycoconjugates of *Mycobacterium tuberculosis*. *Crit. Rev. Biochem. Mol. Biol.* 49, 361–399.

(31) Weber, P. L., and Gray, G. R. (1979) Structural and immunochemical characterization of the acidic arabinomannan of *Mycobacterium smegmatis*. *Carbohydr. Res.* 74, 259–278.

(32) Hunter, S. W., Gaylord, H., and Brennan, P. J. (1986) Structure and antigenicity of the phosphorylated lipopolysaccharide antigens from the leprosy and tubercle bacilli. *J. Biol. Chem.* 261, 12345–12351.

(33) Delmas, C., Gilleron, M., Brando, T., Vercellone, A., Gheorghiu, M., Rivière, M., and Puzo, G. (1997) Comparative structural study of the mannosylated-lipoarabinomannans from *Mycobacterium bovis* BCG vaccine strains: characterization and localization of succinates. *Glycobiology* 7, 811–817.

(34) Guérardel, Y., Maes, E., Briken, V., Chiraf, F., Leroy, Y., Lochter, C., Strecker, G., and Kremer, L. (2003) Lipomannan and lipoarabinomannan from a clinical isolate of *Mycobacterium kansasii*: Novel structural features and apoptosis-inducing properties. *J. Biol. Chem.* 278, 36637–36651.

(35) Gilleron, M., Nigou, J., Cahuzac, B., and Puzo, G. (1999) Structural study of the lipomannans from *Mycobacterium bovis* BCG: characterisation of multiacylated forms of the phosphatidyl-myoinositol anchor. *J. Mol. Biol.* 285, 2147–2160.

(36) Gilleron, M., Bala, L., Brando, T., Vercellone, A., and Puzo, G. (2000) *Mycobacterium tuberculosis* H37Rv parietal and cellular lipoarabinomannans. Characterization of the acyl- and glyco-forms. *J. Biol. Chem.* 275, 677–684.

(37) Nigou, J., Gilleron, M., Brando, T., Vercellone, A., and Puzo, G. (1999) Structural definition of arabinomannans from *Mycobacterium bovis* BCG. *Glycoconjugate J.* 16, 257–264.

(38) Angala, S. K., Li, W., Palcekova, Z., Zou, L., Lowary, T. L., McNeil, M. R., and Jackson, M. (2019) Cloning and Partial Characterization of an Endo- α -(1→6)-d-Mannanase Gene from *Bacillus circulans*. *Int. J. Mol. Sci.* 20, 6244.

(39) Nigou, J., Gilleron, M., and Puzo, G. (2003) Lipoarabinomannans: From structure to biosynthesis. *Biochimie* 85, 153–166.

(40) Slauch, J. M., Lee, A. A., Mahan, M. J., and Mekalanos, J. J. (1996) Molecular characterization of the oafA locus responsible for acetylation of *Salmonella typhimurium* O-antigen: oafA is a member of a family of integral membrane trans-acylases. *J. Bacteriol.* 178, 5904–5909.

(41) Thanweer, F., Tahiliani, V., Korres, H., and Verma, N. K. (2008) Topology and identification of critical residues of the O-acetyltransferase of serotype-converting bacteriophage, SF6, of *Shigella flexneri*. *Biochem. Biophys. Res. Commun.* 375, 581–585.

(42) Thanweer, F., and Verma, N. K. (2012) Identification of critical residues of the serotype modifying O-acetyltransferase of *Shigella flexneri*. *BMC []Biochem.* 13, 13.

(43) Yamazaki, Y., Danelishvili, L., Wu, M., Macnab, M., and Bermudez, L. E. (2006) *Mycobacterium avium* genes associated with the ability to form a biofilm. *Appl. Environ. Microbiol.* 72, 819–825.

(44) Driessen, N. N., Stoop, E. J., Ummels, R., Gurcha, S. S., Mishra, A. K., Larrouy-Maumus, G., Nigou, J., Gilleron, M., Puzo, G., Maaskant, J. J., Sparrius, M., Besra, G. S., Bitter, W., Vandenbroucke-Grauls, C. M., and Appelmelk, B. J. (2010) *Mycobacterium marinum* MMAR_2380, a predicted transmembrane acyltransferase, is essential for the presence of the mannose cap on lipoarabinomannan. *Microbiology* 156, 3492–3502.

- (45) Raetz, C. R. H., Reynolds, C. M., Trent, M. S., and Bishop, R. E. (2007) Lipid A modification systems in Gram-negative bacteria. *Annu. Rev. Biochem.* 76, 295–329.
- (46) Swoboda, J. G., Campbell, J., Meredith, T. C., and Walker, S. (2010) Wall teichoic acid function, biosynthesis, and inhibition. *ChemBioChem* 11, 35–45.
- (47) Needham, B. D., and Trent, M. S. (2013) Fortifying the barrier: the impact of lipid A remodelling on bacterial pathogenesis. *Nat. Rev. Microbiol.* 11, 467–481.
- (48) Schneewind, O., and Missiakas, D. (2014) Lipoteichoic acids, phosphate-containing polymers in the envelope of gram-positive bacteria. *J. Bacteriol.* 196, 1133–1142.
- (49) Torrelles, J. B., Khoo, K. H., Sieling, P. A., Modlin, R. L., Zhang, N., Marques, A. M., Treumann, A., Rithner, C. D., Brennan, P. J., and Chatterjee, D. (2004) Truncated structural variants of lipoarabinomannan in *Mycobacterium leprae* and an ethambutol-resistant strain of *Mycobacterium tuberculosis*. *J. Biol. Chem.* 279, 41227–41239.
- (50) Guerin, M. E., Kaur, D., Somashekar, B. S., Gibbs, S., Gest, P., Chatterjee, D., Brennan, P. J., and Jackson, M. (2009) New insights into the early steps of phosphatidylinositol mannoside biosynthesis in mycobacteria: PimB' is an essential enzyme of *Mycobacterium smegmatis*. *J. Biol. Chem.* 284, 25687–25696.
- (51) McCarthy, R. R., Mazon-Moya, M. J., Moscoso, J. A., Hao, Y., Lam, J. S., Bordi, C., Mostowy, S., and Filloux, A. (2017) Cyclic-di-GMP regulates lipopolysaccharide modification and contributes to *Pseudomonas aeruginosa* immune evasion. *Nat. Microbiol.* 2, 17027.
- (52) Angala, S. K., Palcekova, Z., Belardinelli, J. M., and Jackson, M. (2018) Covalent modifications of polysaccharides in mycobacteria. *Nat. Chem. Biol.* 14, 193–198.
- (53) Rose, S. J., and Bermudez, L. E. (2014) *Mycobacterium avium* biofilm attenuates mononuclear phagocyte function by triggering hyperstimulation and apoptosis during early infection. *Infect. Immun.* 82, 405–412.
- (54) van Kessel, J. C., and Hatfull, G. F. (2007) Recombineering in *Mycobacterium tuberculosis*. *Nat. Methods* 4, 147–152.
- (55) Calado Nogueira de Moura, V., Gibbs, S., and Jackson, M. (2014) Gene replacement in *Mycobacterium chelonae*: application to the construction of porin knock-out mutants. *PLoS One* 9, No. e94951.
- (56) Berg, S., Starbuck, J., Torrelles, J. B., Vissa, V. D., Crick, D. C., Chatterjee, C., and Brennan, P. J. (2005) Roles of the conserved proline and glycosyltransferase motifs of EmbC in biosynthesis of lipoarabinomannan. *J. Biol. Chem.* 280, 5651–5663.
- (57) Gilleron, M., Ronet, C., Mempel, M., Monsarrat, B., Gachelin, G., and Puzo, G. (2001) Acylation state of the phosphatidylinositol mannosides from *Mycobacterium bovis* Bacillus Calmette Guérin and ability to induce granuloma and recruit natural killer T cells. *J. Biol. Chem.* 276, 34896–34904.
- (58) Hawkins, P. T., Stephens, L., and Downes, C. P. (1986) Rapid formation of inositol 1,3,4,5-tetrakisphosphate and inositol 1,3,4-trisphosphate in rat parotid glands may both result indirectly from receptor-stimulated release of inositol 1,4,5-trisphosphate from phosphatidylinositol 4,5-bisphosphate. *Biochem. J.* 238, 507–516.
- (59) Sartain, M. J., Dick, D. L., Rithner, C. D., Crick, D. C., and Belisle, J. T. (2011) Lipidomic analyses of *Mycobacterium tuberculosis* based on accurate mass measurements and the novel Mtb LipidDB. *J. Lipid Res.* 52, 861–872.
- (60) Etienne, G., Villeneuve, C., Billman-Jacobe, H., Astarie-Dequeker, C., Dupont, M.-A., and Daffé, M. (2002) The impact of the absence of glycopeptidolipids on the ultrastructure, cell surface and cell wall properties, and phagocytosis of *Mycobacterium smegmatis*. *Microbiology* 148, 3089–3100.
- (61) Rose, S. J., and Bermudez, L. E. (2016) Identification of Bicarbonate as a Trigger and Genes Involved with Extracellular DNA Export in Mycobacterial Biofilms. *mBio*, DOI: 10.1128/mBio.01597-16.
- (62) Martin, A., Camacho, M., Portaels, F., and Palomino, J.-C. (2003) Resazurin microtiter assay plate testing of *Mycobacterium tuberculosis* susceptibilities to second-line drugs: rapid, simple, and inexpensive method. *Antimicrob. Agents Chemother.* 47, 3616–3619.

SUPPORTING INFORMATION

Polysaccharide succinylation enhances the intracellular survival of *Mycobacterium abscessus*

Zuzana Palčėková¹, Martine Gilleron², Shiva kumar Angala¹, Juan Manuel Belardinelli¹,
Michael McNeil¹, Luiz E. Bermudez^{3,4}, Mary Jackson^{1*}

From the ¹Mycobacteria Research Laboratories, Department of Microbiology, Immunology and Pathology, Colorado State University, Fort Collins, CO 80523-1682, USA; ²Institut de Pharmacologie et de Biologie Structurale, IPBS, Université de Toulouse, CNRS, UPS, 31077 Toulouse, France; ³Department of Biomedical Sciences, College of Veterinary Medicine, Oregon State University, Corvallis, OR 97331, USA; ⁴Department of Microbiology, College of Science, Oregon State University, Corvallis, OR 97331, USA

*Corresponding Author: Mary Jackson; Mary.Jackson@colostate.edu

Table of contents

Table S1: Monosaccharidic composition of LM and LAM from WT *Mabs* ATCC 19977, the Δ *sucT* mutant and the complemented mutant strain.

Table S2: Glycosyl linkage analysis of per-*O*-methylated LM and LAM from WT *Mabs* ATCC 19977, the Δ *sucT* mutant and the complemented mutant strain.

Table S3: Fatty acid composition of the mannosylated phosphatidyl-*myo*-inositol anchor of LM and LAM from WT *Mabs* ATCC 19977 and the Δ *sucT* knockout mutant.

Table S4: Relative percentage of Ara₄ and Ara₆ oligoarabinosides released upon *Cellulomonas gelida* endoarabinanase digestion and the individual representation (%) of covalently modified oligoarabinosides within each group.

Table S5: Monosaccharidic composition of mAGP from WT *Mabs* ATCC 19977, the Δ *sucT* mutant and the complemented mutant strain.

Table S6: Glycosyl linkage analysis of per-*O*-methylated mAGP from WT *Mabs* ATCC 19977, the Δ *sucT* mutant and the complemented mutant strain.

Table S7: Susceptibility of the *Mabs sucT* knock-out mutant to antibiotics and antimicrobial peptides.

Table S8: Translocation of *Mabs* WT, Δ *sucT* and complemented Δ *sucT* mutant strains across polarized monolayers of human A549 lung alveolar type II epithelial cells.

Figure S1: Negative ion liquid chromatography-mass spectrometry (LC-MS) analysis of *Mabs* deacylated PIM₂ (d-PIM₂) and deacylated PIM₆ (d-PIM₆).

Figure S2: Location of the methyl group on *Mabs* tetra-acylated PIM₂.

Figure S3: Absence of capping motifs in *Mabs* LAM.

Figure S4: Primary sequence alignment of SucT from *M. tuberculosis* H37Rv (Rv1565c), *M. smegmatis* mc²155 (MSMEG_3187) and *M. abscessus* ATCC 19977 (MAB_2689) using PSI/TM-Coffee.

Figure S5: Allelic replacement at the *MAB_2689* locus of *Mabs* ATCC 19977.

Figure S6: Congo red does not bind to *Mabs* WT and Δ *sucT* LAM.

Figure S7: Phenotypic characterization of the *Mabs sucT* mutant.

Figure S8: Effect of reactive oxygen species and phagosome acidification on the intracellular replication and survival of the *Mabs sucT* knock-out mutant.

Table S1: Monosaccharidic composition of LM and LAM from WT *Mabs* ATCC 19977, the Δ *sucT* mutant and the complemented mutant strain.

Reported values are averages \pm standard deviations of three technical repeats and represent relative distribution in %.

(A) Monosaccharidic composition of LAM

	<i>Araf</i>	Ino	<i>Manp</i>	2- <i>O</i> -methyl- <i>Manp</i>	<i>Araf/Manp</i>
WT	78.0 \pm 1.2	0.5 \pm 0.1	20.3 \pm 1.4	1.2 \pm 0.3	3.6 \pm 0.3
Δ <i>sucT</i>	81.3 \pm 1.1	0.5 \pm 0.1	17.1 \pm 1.3	1.0 \pm 0.2	4.5 \pm 0.4
Δ <i>sucT</i> comp	78.2 \pm 0.6	0.4 \pm 0.1	19.9 \pm 0.6	1.5 \pm 0.2	3.7 \pm 0.1

The LAMs produced by the three strains show no statistically significant difference in *Araf/Manp* ratio pursuant to the Student's *t*-test ($P < 0.05$).

(B) Monosaccharidic composition of LM

	Ino	<i>Manp</i>	2- <i>O</i> -methyl- <i>Manp</i>
WT	1.5 \pm 0.5	95.6 \pm 1.1	2.9 \pm 0.7
Δ <i>sucT</i>	1.5 \pm 0.6	95.1 \pm 0.5	3.4 \pm 0.7
Δ <i>sucT</i> comp	2.3 \pm 0.5	94.6 \pm 0.6	3.1 \pm 0.2

Table S2: Glycosyl linkage analysis of per-*O*-methylated LM and LAM from WT *Mabs* ATCC 19977, the Δ *sucT* mutant and the complemented mutant strain.

Reported values are averages \pm SD of three technical repeats and represent relative distribution in %.

(A) Glycosyl linkage analysis of per-*O*-methylated LAM^a

	t- <i>Araf</i>	2- <i>Araf</i>	5- <i>Araf</i>	3,5- <i>Araf</i>	t- <i>Manp</i>	6- <i>Manp</i>	3,6- <i>Manp</i> ^b	<i>Araf/Manp</i>	3,6- <i>Manp</i> /6- <i>Manp</i>	2- <i>Araf</i> /5- <i>Araf</i>
WT	9.5 \pm 1.0	6.4 \pm 0.3	45.8 \pm 0.8	14.7 \pm 0.5	10.1 \pm 0.7	7.2 \pm 0.3	6.3 \pm 0.1	3.1 \pm 0.1	0.9	0.14 \pm 0.01
Δ <i>sucT</i>	10.2 \pm 1.3	8.2 \pm 0.5	46.0 \pm 0.8	11.7 \pm 1.1	13.9 \pm 0.4	5.1 \pm 0.5	4.8 \pm 0.3	4.2 \pm 0.5	0.9	0.18 \pm 0.01
Δ <i>sucT</i> comp	14.0 \pm 1.2	8.1 \pm 0.9	37.0 \pm 1.1	14.6 \pm 0.5	10.3 \pm 0.2	7.5 \pm 0.5	8.5 \pm 1.2	2.7 \pm 0.3	1.1	0.22 \pm 0.02

^aThe LAM produced by the three strains show no statistically significant differences in terms of glycosyl linkages of their mannan and arabinan domains pursuant to the Student's *t*-test ($P < 0.05$). ^b2,6 linked *Manp* was found in small variable amounts (less than 16% of the 3,6-*Manp*). We attribute this to under methylation as 2,6-*Manp* could not be detected in the NMR analysis.

(B) Glycosyl linkage analysis of per-*O*-methylated LM^a

	t-Man _p	6-Man _p	3,6-Man _p ^b	3,6-Man _p /6-Man _p
WT	52.3 ± 3.7	20.5 ± 1.7	27.2 ± 2.7	1.3
Δ <i>sucT</i>	55.5 ± 1.0	18.0 ± 1.3	26.5 ± 0.7	1.5
Δ <i>sucT</i> comp	46.0 ± 1.0	20.4 ± 0.6	33.6 ± 0.9	1.6

^aThe LM produced by the three strains show no statistically significant differences in terms of glycosyl linkages of their mannan domain pursuant to the Student's *t*-test (*P* < 0.05). ^b2,6 linked Man_p was found in small variable amounts (less than 16% of the 3,6-Man_p). We attribute this to under methylation as 2,6-Man_p could not be detected in the NMR analysis.

Table S3: Fatty acid composition of the mannosylated phosphatidyl-*myo*-inositol anchor of LM and LAM from WT *Mabs* ATCC 19977 and the Δ*sucT* knockout mutant.

Reported values represent relative distribution in %. TBSA: Tuberculostearic acid.

	C14:0	C15:0	C16:0	C18:1	C18:0	C19:0 (TBSA)
LM WT	0.9	0.7	36.20	6.40	32.9	22.9
LM Δ <i>sucT</i>	1.2	0.4	34.6	1.6	45.8	16.4
LAM WT	14.2	1.5	66.1	1.1	9.1	8.0
LAM Δ <i>sucT</i>	9.0	1.5	57.1	4.8	20.6	7.0

Table S4: Relative percentage of Ara₄ and Ara₆ oligoarabinosides released upon *Cellulomonas gelida* endoarabinanase digestion and the individual representation (%) of covalently modified oligoarabinosides within each group.

	WT	$\Delta sucT$	$\Delta sucT$ comp
Total Ara₄	50.2	38.6	52.4
Unmodified Ara ₄	77	95.8	80.8
Ara ₄ +succinate	14.5	0	13.4
Ara ₄ +acetate	7.6	4.2	5.2
Ara ₄ +succinate+acetate	0.9	0	0.6
Total Ara₆	49.8	61.4	47.6
Unmodified Ara ₆	86.9	98.4	88.3
Ara ₆ +succinate	5.8	0	6.6
Ara ₆ +acetate	7.3	1.6	5.0
Ara ₆ +succinate+acetate	0	0	0.1
SUM	100	100	100

Table S5: Monosaccharidic composition of mAGP from WT *Mabs* ATCC 19977, the $\Delta sucT$ mutant and the complemented mutant strain.

Reported values are averages \pm SD of three technical repeats and represent relative distribution in %. No statistically significant differences between strains were observed pursuant to the Student's *t*-test ($P < 0.05$).

	Rhap	Araf	Gal _f	GlcNAc	MurNAc	Araf/Gal _f	Araf/Rhap	Gal _f /Rhap	mycolic acids/Rhap
WT	1.1 \pm 0.1	46.0 \pm 2.3	22.5 \pm 2.0	10.5 \pm 1.2	15.2 \pm 3.3	2.1 \pm 0.1	43.0 \pm 5.1	20.9 \pm 2.8	25.4 \pm 9.8
$\Delta sucT$	1.2 \pm 0.1	47.8 \pm 1.6	18.9 \pm 1.1	11.2 \pm 2.1	15.7 \pm 3.1	2.5 \pm 0.2	39.5 \pm 0.8	15.7 \pm 1.5	34.6 \pm 3.7
$\Delta sucT$ comp	1.2 \pm 0.3	45.4 \pm 2.1	20.4 \pm 0.9	12.5 \pm 3.9	19.7 \pm 1.0	2.2 \pm 0.1	39.8 \pm 11.5	17.8 \pm 4.9	37.9 \pm 3.8

Table S6: Glycosyl linkage analysis of per-*O*-methylated mAGP from WT *Mabs* ATCC 19977, the Δ *sucT* mutant and the complemented mutant strain.

Reported values are averages \pm SD of three technical repeats and represent relative distribution in %. No statistically significant differences between strains were observed pursuant to the Student's *t*-test ($P < 0.05$).

	t-Araf	2-Araf	5-Araf	3,5-Araf	t-Galf	5-Galf	6-Galf	5,6-Galf	Araf/Galf
WT	7.0 \pm 0.3	6.0 \pm 0.1	36.7 \pm 0.9	9.7 \pm 0.6	3.7 \pm 0.3	20.2 \pm 0.9	11.6 \pm 0.8	4.5 \pm 0.7	1.5 \pm 0.1
Δ <i>sucT</i>	7.6 \pm 0.8	5.3 \pm 0.9	41.5 \pm 3.5	8.2 \pm 1.4	2.8 \pm 0.6	19.1 \pm 1.2	11.2 \pm 1.1	3.8 \pm 0.8	1.7 \pm 0.2
Δ <i>sucT</i> comp	7.2 \pm 0.3	5.8 \pm 0.2	38.2 \pm 0.7	9.5 \pm 0.4	3.1 \pm 0.2	19.3 \pm 0.5	11.4 \pm 0.5	4.6 \pm 0.4	1.6 \pm 0.1

Table S7: Susceptibility of the *Mabs sucT* knock-out mutant to antibiotics and antimicrobial peptides.

MIC were determined in cation-adjusted Mueller-Hinton II broth + 0.05% tyloxapol at 37°C and MIC values are given in $\mu\text{g mL}^{-1}$. AMK, amikacin; APR, apramycin; AZI, azithromycin; CLA, clarithromycin; ERY, erythromycin; KAN, kanamycin; EMB, ethambutol; RIF, rifampicin; STR, streptomycin; CFX, ceftiofur; TOB, tobramycin; LIN, linezolid; TET, tetracycline; IMI, imipenem; CIP, ciprofloxacin. LL-37 (InvivoGen) and HNP-1 (human α -defensin 1; Bachem) are cationic antimicrobial peptides. MIC determinations were performed two times on independent culture batches. nd, not determined.

Antibiotic	<i>Mabs</i> WT	<i>Mabs</i> Δ <i>sucT</i>	<i>Mabs</i> Δ <i>sucT</i> / pMV306- <i>sucT</i>
AMK	10	10	10
APR	2.5	2.5	2.5
AZI	40	80	40
CLA	0.63	0.63	0.63
ERY	5	5	5
KAN	10	10	nd
EMB	>320	>320	>320
RIF	>160	>160	>160
STR	160	160	80
CFX	80	40	80
TOB	40	80	40
LIN	10	5	10
TET	>320	>320	>320
IMI	20	20	20
CIP	5	5	5
LL-37	>100	>100	>100
HNP-1	>100	>100	>100

Table S8: Translocation of *Mabs* WT, Δ *sucT* and complemented Δ *sucT* mutant strains across polarized monolayers of human A549 lung alveolar type II epithelial cells.

No significant difference in translocation after 24 h was observed between mutant and WT or complemented mutant strains ($p>0.05$). Statistical analysis using 2-way ANOVA.

	CFU in the upper chamber	CFU recovered in the basal chamber after 24 h	% of inoculum that translocated after 24 h	Transmembrane potential (Ω/cm^2)
WT	$5.6 \pm 0.6 \times 10^6$	$1.1 \pm 0.8 \times 10^3$	0.020	254
Δ <i>sucT</i>	$5.0 \pm 0.4 \times 10^6$	$8.7 \pm 0.6 \times 10^2$	0.017	246
Δ <i>sucT</i> comp	$4.3 \pm 0.9 \times 10^6$	$8.9 \pm 0.5 \times 10^2$	0.020	251

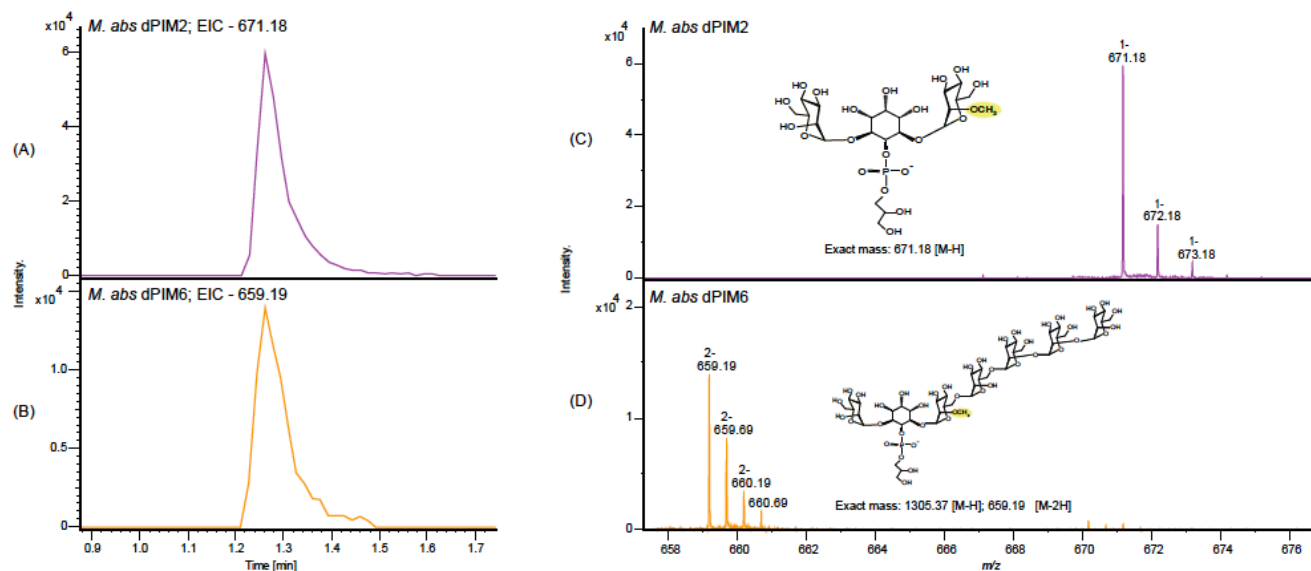


Figure S1: Negative ion liquid chromatography-mass spectrometry (LC-MS) analysis of Mabs deacylated PIM₂ (d-PIM₂) and deacylated PIM₆ (d-PIM₆).

(A, B) Extracted ion chromatograms (EICs) for d-PIM₂ (A) and d-PIM₆ (B) with m/z values of 671.18 and 659.19, respectively. (C, D) The mass spectra showing the singly charged [M-H] for d-PIM₂ (C), and doubly charged [M-2H] for d-PIM₆ (D). The chemical structures with exact mass corresponding to the methylated forms of d-PIM₂ (C) and d-PIM₆ (D) are shown.

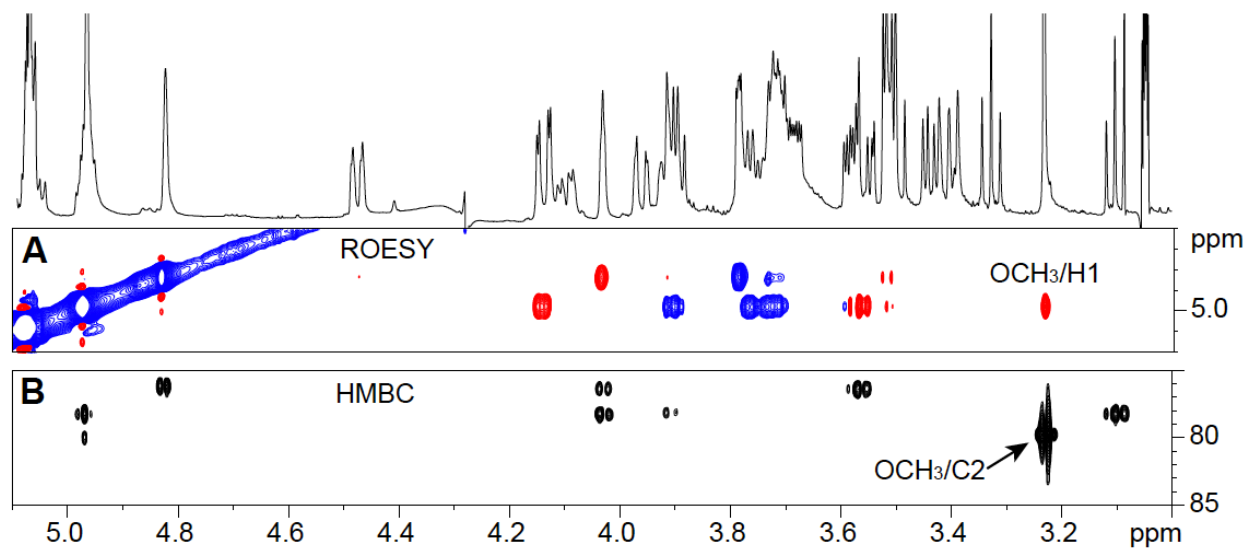


Figure S2: Location of the methyl group on *Mabs* tetra-acylated PIM₂.

Expanded regions of the 2D ^1H - ^1H ROESY (δ ^1H 5.10-3.00 and δ ^1H 5.20-4.60) (A) and of the 2D ^1H - ^{13}C HMBC (δ ^1H : 5.10-3.00, δ ^{13}C 85-75) (B) NMR spectra of the Ac₂PIM₂ from WT *Mabs* ATCC 19977 in CDCl₃/CD₃OD/D₂O, 60:35:8 (v/v/v) at 298 K.

On the ROESY spectrum (A), noe contacts are in red, while cosy contacts are in blue. The two important cross peaks allowing the location of the methyl group are annotated.

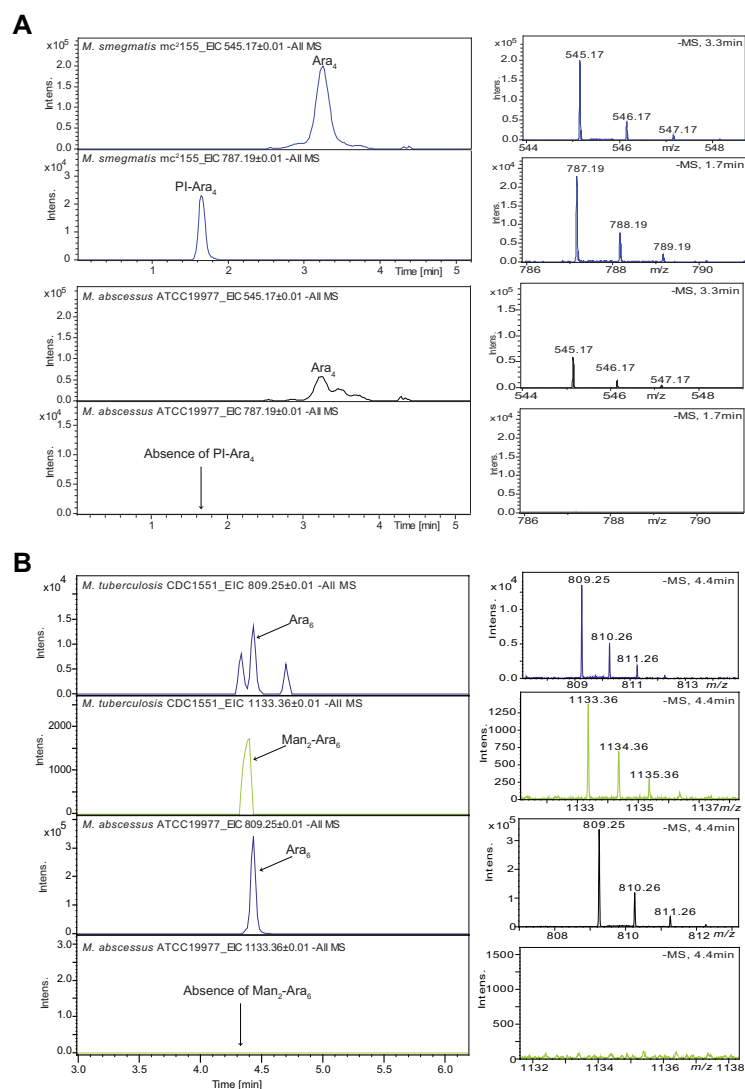


Figure S3: Absence of capping motifs in *Mabs* LAM.

The most abundant capped digestion product cleaved by *Cellulomonas gelida* endoarabinanase from the nonreducing end of LAM from *M. smegmatis* (A) and *M. tuberculosis* (B) is, respectively, phosphoinositol-Ara₄ with an exact mass of m/z 787.1915 $[M-H]^-$ and Man₇-Ara₆ with an exact mass of m/z 1133.36 $[M-H]^-$. None of these ions were detected in digested *Mabs* LAM (panels A and B). Three signals at similar retention times with an exact mass of m/z 545.1723 $[M-H]^-$ corresponding to Ara₄ were found in the digested *Mabs* LAM which reveals the possibility of more structural isomers of tetraarabinosides released by *Cellulomonas gelida* endoarabinanase.

IN	HEL	OUT		
Rv1565c	1	MLTLSP--RPPALTPEPALPPVTMGTRTTGFYRHDI DGI RGVATAI VAVFHVWFGVRSGGVDVFI AI	66	
MSMEG 3187	1	-----PSMGRKSGFYRHDI DGI RGTATMMVAVFHTWFGVRSGGVDVFI AI	46	
MAB_2689	1	MFFVSATKPTKDPEVSPAAMDATPKPKGDKAFYRYDLGLRGIAIFLVAVFHVWFGVRSGGVDVFLTL	69	
	1	*****	69	
Rv1565c	67	SGFFGGKILRAALNPDLSLSPAIEVIRLIRLLPALVVVLVLAGCALLTIAIOPOTRWEAFANOSLASLG	135	
MSMEG 3187	47	SGFFGGKILRTALDOSTPLRLSEVVRVIRLLPALVVVLAANAALVILIPOTRWEAFADOSLASLG	115	
MAB_2689	70	SGFFYGSKLLRTATTQASLNPPVVKRLVIRLLPALILVLAACAVLTVLVQPETRWETFAEQSLASLG	138	
	70	*****	138	
Rv1565c	136	YYONWFI ASTVSNYI RAGFAVSPi OHTWSMSVQGFYI AFI I I VAGCAYI I RRLFRGPRAPYI RTMFVV	204	
MSMEG 3187	136	YYONWFI ANTAADYI RAGFTVSPi OHTWSMSVQGFYTAI VI TFGFAYI FRR----VFGRHIRTFTV	180	
MAB_2689	119	YYONWELANTADYLAASESVSPLOHLWSMSVQGFYVGLVALVYLLAVLLRK----PLGRHIRTVLIV	207	
	139	*****	207	
Rv1565c	205	LLSTLTLASFIYAI VAHHAYOATAYNTFARAWELLGALVGAVPVHVRWPMWLRTAVATAALAAILSC	273	
MSMEG 3187	181	LLAALTIASFYVYIAHTNTDOATAYNSFARAWELLGALGALVGFVRWPMWLRTVSVVSLAAILSC	249	
MAB_2689	204	VIAVLSAASFYAIYAHLDQSIAYNTFARAWELLGLVLGALVAGTRWPRWLROLLSFAVAVAILSC	272	
	208	*****	276	
Rv1565c	274	GAI TDGVKFFPGPWAI VPVGATMI MTI AGANROGHPGTRDRi PI PNRI I ATAPI VAI GAMAYSWYI WHW	342	
MSMEG 3187	250	GWFTDGVKFFPGPWAI VPVGATTI FTFSANRMSDPRTAGRI PAPNRI I ATAPFVSI GSMAYSI YI WHW	318	
MAB_2689	273	GALINGVREFPGPLALVPVATLTLTSAANLPSD---ARQPVNRFPLATRLVELGALAYSLYLWHW	337	
	277	*****	345	
Rv1565c	343	PLLIFWLSYTGHRHANFVEGAALLVSGLLAYLTTRLVEDPLRYRAPAGVRSPAAPVPIPWRLRLRRPT	411	
MSMEG 3187	319	PLLIFWLSYSGHTAANFVEGAVILLVSGVLAWLTTRYIEEPLRTOGP-----RAPVPAVPLRARLRRPT	382	
MAB_2689	338	PLLVLWLVYTGEARVTVAEGAAILGLSLALAYLTNKYIETPLRYP-R-----VSPT-SASLWTLRLRRPT	399	
	346	*****	414	
Rv1565c	412	TVI GSVVAI I GVAI TATSFTRWFHVTVORAAGKFI SGI SSRDYPGARAI TDHVRVPKI RMRPTVI FVRH	480	
MSMEG 3187	383	TVI GSTVAI I GVAI TATSFTRWFHVTVORAAGKFI SGI SARDYPGARAI TDHARVPKI PMRPTVI FAKN	451	
MAB_2689	400	LALGTSIVLMAVALTATSFTELEHVTVQRSNGKELSGLRPRDYPGAGALLYGDVRDPLPMRPTTLEASD	468	
	415	*****	483	
Rv1565c	481	DLPTSTKDGCIISDFVNPAIINCTYGDVDAPRTIALAGGSHAEHWLTALDILLGRMHFKVVTYLYKMGCP	549	
MSMEG 3187	452	DIPISTTFGCIISDFANVGVINCTYGDKNATRTTIAI AGGSHAFHWTTIAI DI I GOKHGFKVVTYLYKMGCP	520	
MAB_2689	469	DLPTTTEQDCIISDFRNRVITCTYGNPHATRTIALAGGSHAEHWITALDILGRQHNFKITTYLYKMGCP	537	
	484	*****	552	
Rv1565c	550	STEEVPLIMGNNAYPPOCHOWVOAAMAKLADHPDYFTTSTRPW- IKPGDVMPATYVGIWOTFADNN	617	
MSMEG 3187	521	STEEVPLVSGDNRPYPKCHEWNORVMAKLIADHPDYFTTSTRPW- IKPGDVMPSTYLGIEWTFENNN	588	
MAB_2689	538	STEEVPRIAGSNDPYPDCKKWVDEVMRSRIIEQHPDYFTTITRPRSALGDGDMVPESYLGWISAFDEAG	606	
	553	*****	621	
Rv1565c	618	TPVI AMRDTPWV V-KDGPFTPADCI AKGNGNPOSCGTARSKVI VDRNPIT DFVARFPI I KPI DMSDATC	685	
MSMEG 3187	589	TPVI AMRDTPWV T-RNGKPYFPADCI AGGDGAVSCGVKRSKVI SDRNPTI DYI DRFPI MKPI DMSDAVC	656	
MAB_2689	607	TPVLGMRDPTWLIDKGTITYADCSAGGATDCAMDRNALDDVNPTLAIANRFLTKILDMDATC	675	
	622	*****	690	
Rv1565c	686	RTDTCRAVEGNVLVYRDSHHLLTPTYMRMTSELGROIAAANTDWW----- 729		
MSMEG 3187	657	REDHCRVVEGNVLVYHDSHHLSATYMRMTNELGROMAAATGWW----- 700		
MAB_2689	676	RPDKCRVVEGNVLVYHDSHHISATYMRMTAKELGRQIALATGWRRPAQPGQ 726		
	691	***** 741		

Conserved sequence (*), conservative mutations (:), semi-conservative mutations (.), and non-conservative mutations (). Predicted essential functional residues for catalytic activity are boxed in green.

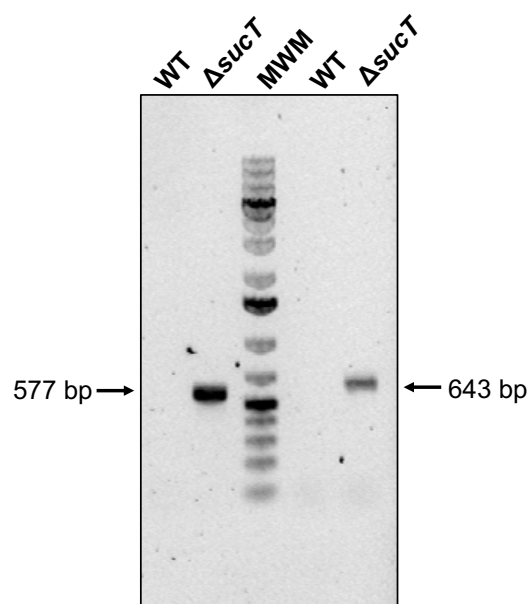


Figure S5: Allelic replacement at the *MAB_2689* locus of *Mabs* ATCC 19977.

Allelic replacement at the *MAB_2689* locus was confirmed by PCR using sets of primers located outside the allelic exchange substrates and inside the zeocin resistance cassette. The expected sizes of the PCR amplification products in the knock-out mutant are 577-bp for the upstream region of the deleted gene and 643-bp for the downstream region. No amplification was expected in the WT parent strain.

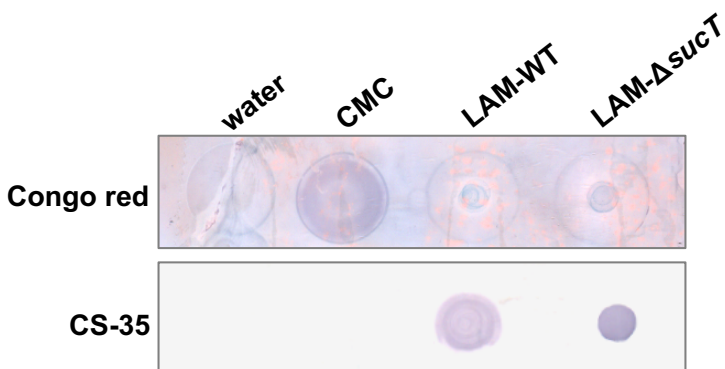


Figure S6: Congo red does not bind to *Mabs* WT and Δ *sucT* LAM.

Equal amounts of LAM from the WT and Δ *sucT* mutant strains were dot-blotted on the nitrocellulose membrane and stained with Congo red. Carboxymethylcellulose (CMC) (same amount loaded as for LAM) was used as a positive control for Congo red binding. LAM from the WT and mutant strains failed to react with Congo Red while they reacted, as expected, with the anti-LAM antibody CS-35.

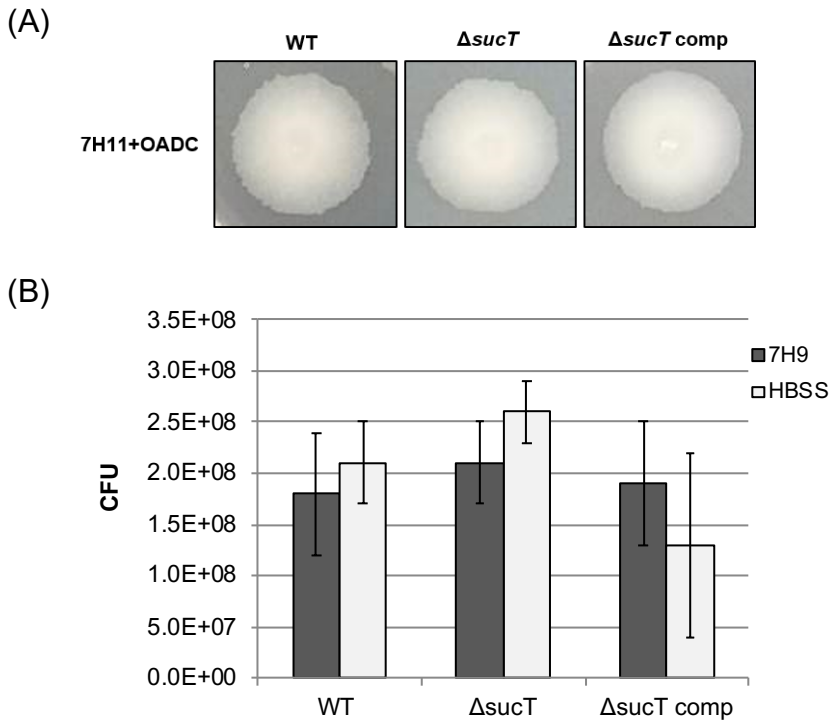


Figure S7: Phenotypic characterization of the *Mabs sucT* mutant.

(A) Colony morphology of WT *Mabs* ATCC 19977, the $\Delta sucT$ mutant and the complemented mutant strain after 3 day of incubation on 7H11-OADC agar at 37°C.

(B) Comparison of the ability of WT *Mabs* ATCC 19977, the $\Delta sucT$ mutant and the complemented mutant strain to form static biofilms in Hank's balanced salt solution (HBSS) and 7H9-OADC culture medium.

No statistically significant differences in biofilm formation, neither in 7H9-OADC or HBSS buffer, were observed between strains pursuant to Student's *t*-test ($P < 0.05$).

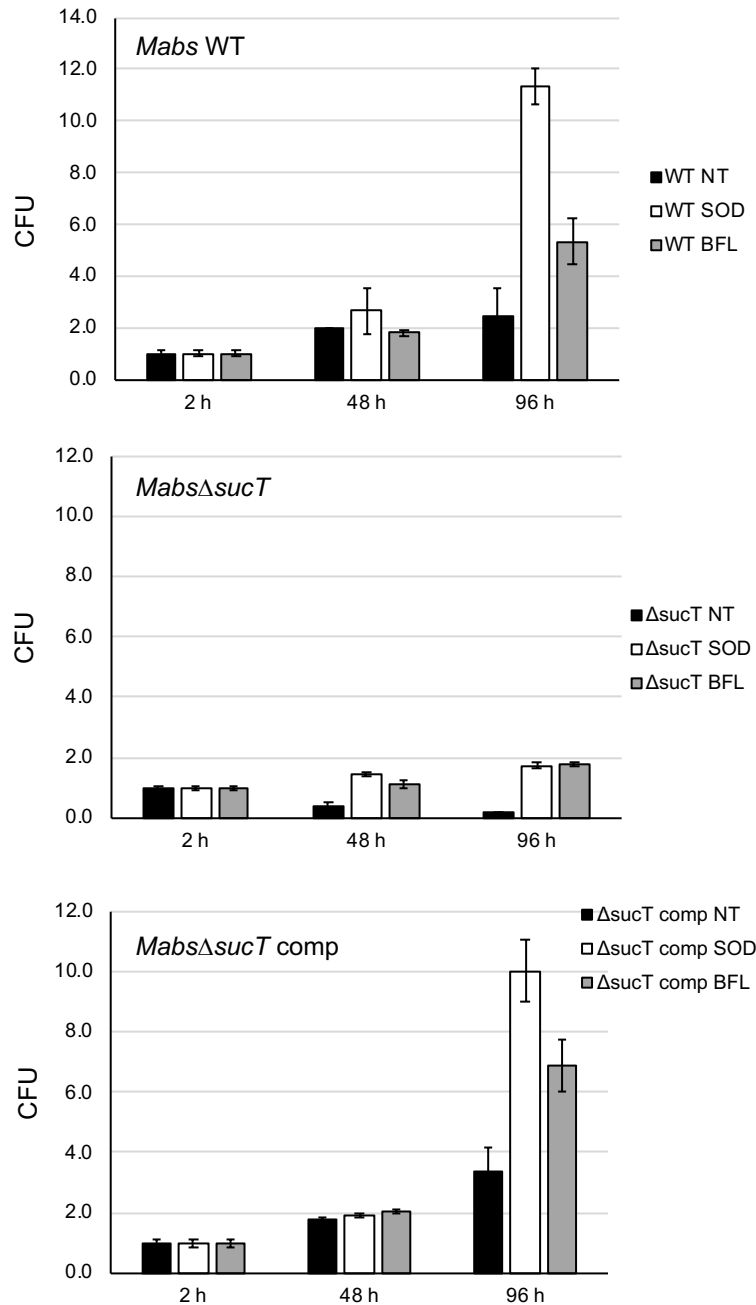


Figure S8: Effect of reactive oxygen species and phagosome acidification on the intracellular replication and survival of the *Mabs sucT* knock-out mutant.

Infected THP-1 macrophages were either non-treated (NT) or treated with superoxide dismutase (SOD) to inhibit superoxides, or treated with bafilomycin A1 (BFL) to inhibit vacuolar acidification. Intracellular CFU over time (average \pm SD of triplicate wells) were enumerated and are expressed relative to the number of CFU two hours post-infection for each treatment group arbitrarily set to 1. The results presented are representative of three independent experiments.